Journal of the Neurological Sciences 478 (2025) 123735

Contents lists available at ScienceDirect

Journal of the Neurological Sciences

journal homepage: www.elsevier.com/locate/jns

Review Article

Deep Learning in neuroimaging for neurodegenerative diseases: State-of-the art, Challenges, and Opportunities

Taymaz Akan [a,b], Sara Akan [c], Sait Alp [d], Christina Raye Ledbetter [e], Ahmad P. Tafti [f], Octavio Arevalo [g], Mohammad Alfrad Nobel Bhuiyan [a,*]

[a] Department of Medicine, LSU Health Shreveport, Shreveport, LA, USA
[b] Department of Software Engineering, Faculty of Engineering, Istanbul Topkapı University, Istanbul, Türkiye
[c] Department of Computer Engineering, Faculty of Engineering, Istanbul Galata University, Istanbul, Türkiye
[d] Department of Artificial Intelligence Engineering, Trabzon 61335, Turkey
[e] Department of Neurosurgery, LSU Health Shreveport, Shreveport, LA, USA
[f] School of Health and Rehabilitation Sciences, University of Pittsburgh, Pittsburgh, PA, USA
[g] Department of Radiology, LSU Health Shreveport, Shreveport, LA, USA

ARTICLE INFO

Keywords:
Deep learning
Neurodegenerative diseases
Brain disorders
Brain volume
3D brain scans
CNN
Transformers
Neuroimaging modalities
Early diagnosis

ABSTRACT

Neuroimaging is commonly used to diagnose neurodegenerative diseases (NDDs), providing crucial insights into brain changes before clinical symptoms manifest. Deep learning (DL) for neuroimaging can improve early diagnosis and disease monitoring. Clinical implementation of DL faces challenges in accurately representing real-world data. Recent models, particularly those focused on diagnostic categorization, have achieved high accuracy, but their applicability to patients is limited. Conflicting inferences have been reported, with findings from small cohorts generalizing conclusions without considering inter-scanner, intra- and inter-site variations. A theoretically feasible method involves gathering a comprehensive dataset that encompasses all patient demographics, but this presents practical challenges including harmonization, data incompleteness, class imbalance, and substantial costs. Existing research has also mostly focused on common NDDs like Alzheimer's Disease (AD) and Parkinson's Disease (PD). This contribution expands the literature by looking at a wider range of NDDs, exploring the latest advancements in applying deep learning algorithms to neuroimaging analysis for the diagnosis and monitoring of NDDs, including AD, Frontotemporal Dementia (FTD), Lewy Body Dementia, PD, Huntington's Disease, Amyotrophic Lateral Sclerosis, and Multiple Sclerosis. We emphasize how these approaches are handling spatial/temporal information available in brain volume imaging data. We conclude by discussing the challenges associated with the use of voxel-based, patch-based, ROI-based, and slice-based approaches in brain volume imaging. These challenges are further compounded by issues such as inter-site and inter-scanner variability, class imbalances in medical datasets, and the scarcity of accurately annotated data, all of which impact the performance and generalizability of deep learning models.

1. Introduction

Neurodegenerative diseases (NDDs) are progressive disorders characterized by neuronal degeneration, resulting in the deterioration of brain function and ultimately death [1]. NDDs are defined by a clinical syndrome of neurological abnormalities, behavioral alterations, increasing functional deterioration, and motor difficulties, all stemming from irreversible neuronal death.

While quantifying the number of NDs presents a significant challenge due to many remaining unclassified and overlapping in clinical features, potentially leading to classification into various classes and subclasses [2], there are over 600 NDs. While some are well-known and well-studied, many are rare affecting only a small number of individuals worldwide [3]. Several of the most prevalent NDDs have been extensively studied and categorized (see **Table 1**). These diseases involve selective neuronal vulnerability, degeneration in specific brain regions, and abnormal protein deposits in neurons and other cells [4–6]. Gerstmann-Sträussler-Scheinker (GSS) disease, Kuru disease, Spinocerebellar ataxia (SCA), and autism spectrum disorder (ASD) are all classified as neurodegenerative disorders. However, they are not among the most

* Corresponding author.
E-mail address: nobel.bhuiyan@lsuhs.edu (M.A.N. Bhuiyan).

https://doi.org/10.1016/j.jns.2025.123735
Received 27 August 2025; Received in revised form 1 October 2025; Accepted 21 October 2025
Available online 24 October 2025

Table 1
Overview of most common NDDs: This table summarizes the nine prominent NDDs, highlighting the diversity in their mechanisms of action and the range of symptoms they cause.

Disease	Associated Proteinopathy	Primary Features	Impact
Alzheimer's Disease (AD)	Amyloid-Beta, Tau	Accumulation of amyloid plaques and neurofibrillary tangles	Cognitive decline, dementia
Frontotemporal Dementia (FTD)	TDP-43, Tau	Degeneration of the frontal and temporal lobes of the brain	Changes in personality, behavior, and language
Lewy Body Dementia (DLB)	Alpha-synuclein	Presence of Lewy bodies, affecting cognition, behavior, and movement	Cognitive impairment, parkinsonism, autonomic dysfunction
Parkinson's Disease (PD)	Alpha-synuclein	Motor symptoms, loss of dopaminergic neurons, presence of Lewy bodies	Tremors, stiffness, movement difficulties
Huntington's Disease (HD)	Huntingtin protein	Genetic mutations leading to neurodegeneration, affecting movement, cognition, emotions	Movement disorders, cognitive decline, emotional disturbances
Amyotrophic Lateral Sclerosis (ALS)	TDP-43	Degeneration of motor neurons, leading to muscle weakness and paralysis	Muscle weakness, paralysis, loss of mobility
Multiple Sclerosis (MS)		Attack on the central nervous system, disrupting information flow	Neurological symptoms, potential disability

common NDDs.

NDDs typically exhibit preclinical, mild, and fully developed clinical manifestations, despite the differences in phenotypes [3]. Early diagnosis is critical in NDDs because it allows for intervention before the disease progresses from preclinical to mild, and eventually to fully developed clinical stages. This early intervention is crucial as it creates an opportunity to substantially reduce or modify the disease's effects on the brain and its functions, perhaps averting or postponing progression to more severe stages.

The diagnosis of neurodegenerative diseases utilizes a multifaceted approach that incorporates neuroimaging methods, evaluations of motor function, study of linguistic characteristics, molecular and genetic information, and an examination of clinical records [7]. NDDs are increasingly being investigated by computed tomography (CT), positron emission tomography (PET), and magnetic resonance imaging (MRI), which includes high-resolution anatomical imaging (T1), diffusion tensor imaging (DTI), and functional MRI. These advanced techniques can identify the signature of each neurodegenerative disorder, facilitating diagnosis and disease progression tracking. These techniques range from eye inspection to more complicated procedures including brain volume measures, diffusion tensor MRI, and functional MRI, allowing researchers to investigate many aspects of neurodegeneration and design tailored therapeutics [8].

The rapid increase of NDDs highlights the necessity for innovative techniques to improve early and precise diagnosis, which is crucial for managing their effects on mortality, disability, and life expectancy. Precise diagnosis is essential for the proper management and treatment of neurodegenerative diseases. It not only provides diagnostic and prognostic information to patients, but it also optimizes treatment strategies, facilitates care, and allows patients to participate in clinical trials. Misdiagnosis can result in ineffective care and costly investigations [9].

Early diagnosis of NDDs is difficult because symptoms do not appear until significant neuron loss has occurred, resulting in increased research into computer-aided diagnosis (CAD) systems for early diagnosis [7]. A CAD system can be divided into conventional machine learning (ML) and deep learning-based methods. Thanks to the availability of large data sets and advancements in computing power, deep learning has significantly resurrected machine learning [10–15]. Most conventional approaches employ a four-stage pipeline of preprocessing, segmentation, feature extraction, and classification [16]. On the other hand, deep learning (DL) algorithms require little or no image preprocessing. They can automatically infer an optimal data representation from raw images without requiring prior feature selection, resulting in a more objective and less biased process. Conventional methods use hard-to-get handcrafted features. Consequently, DL algorithms are more appropriate for detecting fine and diffuse anatomical abnormalities. Deep learning has the potential to aid in diagnosis, develop new therapies, and enhance our comprehension of disease progression.

DL techniques have the ability to uncover hidden patterns in large datasets that were previously invisible. Recent advances in deep learning techniques have shown that these methods can "see the unseen" in videos and images. Consequently, DL techniques are potentially able to perform automatic diagnosis without knowledge awareness. Deep learning algorithms can transform massive amounts of data into actionable insights by utilizing medical imaging sources such as MRI, CT, DTI, PET, and X-ray. This capability improves not only the precision and accuracy of disease detection and categorization, but also the ability to predict disease progression and outcomes. Furthermore, deep learning enhances the segmentation of complex imaging data, allowing for more comprehensive analysis and comprehension of disease mechanisms, potentially resulting in tailored treatment strategies and enhanced patient care.

This review aims to synthesize and expand on the existing body of research on NDDs by focusing on the most recent advancements in neuroimaging techniques and the incorporation of deep learning models to improve the diagnosis, monitoring, and understanding of these complex conditions. While several review papers have looked at different aspects of NDDs separately or with different data types [17–19], this paper focuses on the potential of 3D neuroimaging modalities and deep learning algorithms for improving early diagnosis and disease monitoring in the most common NDDs. This review paper aims to fill significant gaps in the current literature, which is primarily concerned with common NDDs such as AD and PD, by providing a comprehensive overview of a broader range of NDDs, including but not limited to FD, DLB, HD, ALS, and MS. This review's most notable feature is its thorough examination of the various neuroimaging modalities used in the diagnosis and monitoring of these diseases. Additionally, this paper explores the diverse data types utilized in brain imaging, with a particular emphasis on the methodologies and obstacles associated with each, particularly volumetric imaging data. It also contains a comprehensive list of available 3D image datasets for each discussed NDD, which are invaluable resources for future research. This review paper meticulously catalogues the tools and libraries required for brain image analysis and pre-processing. It also aims to bridge the gap between traditional data analysis techniques and modern, automated data handling methods, particularly for temporal and longitudinal data, by providing comprehensive resources for both researchers and clinicians. The paper discusses the applications of deep learning in various neurodegenerative diseases, emphasizing the potential of artificial intelligence in medical imaging and indicating future avenues for substantial advancements in the early detection and treatment of these conditions.

Our literature review methodology used a targeted approach, with publications chosen based on their relevance as determined by the scholar. Google's search engine focuses on high-impact and recent contributions from the last five years. We only included studies from prestigious journals and renowned conferences, such as CVPR, to ensure that our review includes the highest quality and most relevant research

from this rapidly evolving field.

2. Neurodegenerative diseases

Neurodegenerative diseases, including AD, FTD, LBD, PD, HD, ALS, and MS, affect millions globally, presenting distinct patterns of progression and diagnostic challenges. These conditions are characterized by chronic, progressive damage to specific brain regions, leading to cognitive, behavioral, and motor impairments, as well as the dysfunction and eventual death of neural cells in the brain and spinal cord [20,21].

2.1. Prevalence, symptoms, and progression of NDDs

The prevalence of neurodegenerative diseases varies considerably. AD is the most common, with an estimated 50 million cases worldwide in 2015, which are expected to triple by 2050 [20,22,23]. FTD is less common, affecting only 4 to 15 people per 100,000, with the majority of them being under the age of 65 [24–26]. LBD impacts about 1.4 million individuals in the U.S., accounting for 3.8% of new dementia diagnoses [27,28] PD, the second most prevalent neurodegenerative disorder, is becoming more prevalent, particularly in aging populations. In contrast, HD is rare, with an estimated 1 in 10,000 to 1 in 20,000 individuals affected, typically between the ages of 30 and 50 [29] According to projections, the incidence of ALS is expected to rise from 9.9 per 100,000 individuals in 2022 to 10.5 per 100,000 individuals by 2030 [30]., MS affects more than 2.5 million individuals worldwide, with a higher incidence among women [31].

The symptoms of various conditions frequently overlap, despite their diversity. AD is characterized by cognitive decline, personality changes, and memory loss [32]. Behavioral and personality changes, language deficits, and psychiatric symptoms are all characteristics of FTD [33–36]. Visual hallucinations, cognitive fluctuations, parkinsonism, and REM sleep behavior disorder are all characteristics of LBD [37,38]. Motor symptoms, including tremors, stiffness, and bradykinesia, as well as non-motor symptoms, including mood disorders, are all manifestations of Parkinson's disease [39]. Choreatic movements, progressive cognitive decline, and psychiatric disturbances are all components of HD [29,40]. Progressive muscle weakness and atrophy are frequently observed in ALS, which is frequently accompanied by respiratory insufficiency [41–43]. In contrast, MS is characterized by sensory disturbances, motor dysfunction, and cognitive impairment as a result of CNS lesions [44,45].

These diseases progress through distinct phases. AD begins in the preclinical stage, progresses to mild cognitive impairment, and eventually leads to dementia [46] FTD and LBD frequently exhibit subtle early symptoms, which lead to more noticeable cognitive and behavioral deficits [47,48]. PD progresses from unilateral motor symptoms to severe bilateral impairment and loss of independence [49]. HD has three stages: at-risk, preclinical, and clinical, with gradual motor and cognitive decline [50–53]. MS progresses from clinically isolated syndrome (CIS) to relapsing or progressive phases [54].

2.2. Neuroimaging in Neurodegeneration

Neuroimaging is crucial for the diagnosis, differentiation, and management of NDDs, as it reveals structural, functional, and metabolic alterations in the brain. Various imaging modalities are used to identify disease-specific patterns, track progression, and guide early intervention strategies.

Magnetic Resonance Imaging (MRI) can be utilized for both sMRI (Structural MRI) and fMRI (Functional MRI) based on the particular application. sMRI is an essential diagnostic instrument, providing high-resolution images of cerebral anatomy via T1- and T2-weighted sequences. It can detect structural anomalies such as medial temporal lobe atrophy in Alzheimer's disease, dementia with LB, Parkinsonian syndromes, multiple system atrophy, and HD [55–67].

fMRI is an efficient technique for investigating brain function by identifying changes in blood flow via blood-oxygen-level-dependent contrast. It quantifies regional cerebral blood flow as an indicator of neuronal activity, offering insights into the brain's functional organization and its modifications in NDDs [62]. Task-based fMRI delineates functional impairments and compensatory strategies by mapping active regions during designated tasks, whereas resting-state fMRI uncovers disturbances in intrinsic connectivity networks. In Alzheimer's disease, fMRI studies demonstrate diminished activation in memory-associated regions and impaired connectivity within the default mode network, which may function as early biomarkers. In DLB, fMRI demonstrates diminished activation of the visual cortex and impaired connectivity with the posterior cingulate cortex, distinguishing DLB from AD [68]. In PD, fMRI reveals modified activation in the basal ganglia and motor networks during motor tasks, as well as disturbances in fronto-striatal circuits during cognitive tasks, illuminating both motor and non-motor symptoms [62,69].

Chemical Exchange Saturation Transfer (CEST) MRI is a sophisticated imaging modality that improves contrast in MRI images by utilizing the proton exchange between water and various molecules within tissue. This method can yield distinctive insights into the biochemical and molecular milieu within tissues, which conventional MRI techniques may overlook [70].

Fluid-Attenuated Inversion Recovery (FLAIR) imaging is especially effective for detecting white matter lesions and abnormalities adjacent to cerebrospinal fluid (CSF) areas by attenuating free fluid signals. It is frequently utilized in the diagnosis of multiple sclerosis and other neurodegenerative conditions characterized by demyelination, ischemia, or inflammation [71]. FLAIR enhances T1- and T2-weighted images by improving the visibility of lesions in white matter.

Single-Photon Emission Computed Tomography (SPECT) is an imaging modality that offers significant insights into cerebral function, particularly in NDDs. This method is frequently employed to examine the distribution of dopamine transporters in the brain, aiding in the differentiation of various parkinsonian syndromes. SPECT imaging can distinguish between PD and Multiple System Atrophy by revealing distinct patterns of dopamine transporter depletion. [72]. It is utilized to evaluate regional cerebral blood flow, indicative of neural activity, thereby aiding in the comprehension of the functional organization of the basal ganglia and its projections. This imaging technique is essential for both diagnosis and the assessment of disease progression and therapeutic efficacy. SPECT may reveal bilateral temporoparietal and posterior cingulate hypoperfusion, facilitating the diagnosis and differentiation of AD from other dementias [73,74]. SPECT imaging of cerebral blood flow offers critical diagnostic insights and aids in monitoring disease progression and therapeutic response.

Positron Emission Tomography (PET) is a significant imaging technique for monitoring metabolic processes in the body. PET is especially useful in identifying areas of the brain with reduced glucose metabolism in NDDs. It is important in the study of PD, HD, and AD. PET scans with tracers like [18F]-FDG can help distinguish AD from other atypical parkinsonian syndromes such as multiple system atrophy (MSA) and progressive supranuclear palsy (PSP) [75,76]. These scans evaluate presynaptic dopaminergic function, which helps with early detection and disease progression. PET can also detect early metabolic changes in the caudate and putamen, which correlate with disease severity and progression. This enables disease detection and intervention at an early stage. PET imaging may reveal metabolic patterns characteristic of HD, facilitating early diagnosis and differentiation of AD from other dementias. PET imaging utilizing amyloid-specific tracers can identify amyloid plaques, a defining characteristic of AD, essential for early diagnosis and possible therapeutic intervention [77].

Magnetic Resonance Spectroscopy (MRS) is a crucial tool for studying NDDs since its inception in the 1980s. It evaluates brain parameters like tissue metabolism, blood-brain barrier integrity, and

neurotransmitter function [78]. MRS is special because it can detect many brain chemicals in living people. It is like an advanced MRI that looks at brain chemicals instead of just pictures. The most common chemicals it looks at are protons, phosphorus, and carbon. Proton MRS is the most used because it can detect important brain chemicals like N-acetylaspartate (NAA), choline (Cho), and creatine (Cr) [79]. These chemicals help in diagnosing diseases like AD and HD [80–82]. In AD, Proton MRS often shows higher myo-inositol and lower NAA levels, helping to tell Alzheimer's apart from other brain diseases [83]. Phosphorus MRS measures energy-related chemicals in the brain, such as adenosine triphosphate (ATP) and phosphocreatine (PCr) [84]. Proton MRS is a tool that detects brain chemical changes in Alzheimer's, Huntington's, and Parkinson's diseases, aiding in disease progression and testing new treatments. It also identifies early changes in brain metabolism, enhancing our understanding of these conditions.

Understanding the invasiveness and applications of various brain imaging techniques requires distinguishing between non-invasive and minimally invasive methods. MRI and MRS are non-invasive imaging techniques. The detection of structural abnormalities, such as brain injuries and tumors, is facilitated by the generation of detailed images of the brain using strong magnetic fields and radio waves in MRI. The concentration of specific chemicals in the brain is measured by MRS, an extension of MRI, which aids in the diagnosis of NDDs and reveals information about brain metabolism. Conversely, PET and SPECT necessitate the injection of radioactive tracers, rendering them minimally invasive procedures. PET is employed for functional imaging to evaluate brain metabolism, blood flow, and neurotransmitter activity, rendering it advantageous for the diagnosis and monitoring of conditions such as AD, PD, and HD. SPECT also provides functional imaging by utilizing gamma rays and tracers to assess blood flow and neurotransmitter receptors, which aids in the diagnosis of conditions such as epilepsy, stroke, and NDDs. **Table 2** provides a detailed comparison of these imaging techniques, emphasizing their descriptions, invasiveness levels, and main applications. **Figure 1** adds to this overview by visually presenting representative brain images produced by each modality, allowing direct comparison of their spatial and contrast properties.

Table 2
Invasiveness and Applications of Brain Imaging Techniques

Imaging Technique	Description	Invasiveness	Applications
sMRI	Uses strong magnetic fields and radio waves to generate detailed images.	Non-invasive	Structural imaging for detecting tumors, brain injuries, and NDDs.
fMRI	Measures and maps brain activity by detecting changes in blood flow.	Non-invasive	Observing brain function, understanding mental processes.
DTI	Measures the diffusion of water molecules in tissue to map white matter tracts in the brain.	Non-invasive	Analyzing white matter integrity; useful in traumatic brain injury, stroke, and neurodevelopmental or neurodegenerative disorders.
CEST MRI	Detects exchange of protons between water and other molecules to provide cellular environment information without external contrast agents.	Non-invasive	Used in oncology, neurology, and ADresearch to highlight molecular concentration changes.
FLAIR MRI	MRI sequence that nullifies fluid signals to enhance contrast of lesions and abnormalities in the brain.	Non-invasive	Identifies lesions in multiple sclerosis, inflammation, infection, and cancer in clinical diagnostics.
PET	Uses radioactive materials (tracers) to visualize metabolic processes.	Minimally invasive	Functional imaging for assessing brain metabolism, blood flow, and neurotransmitter activity.
SPECT	Uses gamma rays and radioactive tracers to create volumetric brainimages.	Minimally invasive	Functional imaging for evaluating blood flow and neurotransmitter receptors.

3. Data types in brain imaging

Brain imaging techniques generate a wide range of data types that are necessary for understanding the brain's structure and function. Structural imaging techniques such as MRI and DTI generate high-resolution 3D anatomical images and diffusion tensor maps, respectively, which are used to visualize brain structure, detect abnormalities, and investigate brain connectivity. Functional imaging techniques, including fMRI, PET, and SPECT, generate time-series data that reflect variations in blood oxygenation, tracer concentration, and gamma radiation emission, respectively. These data types facilitate the mapping of brain activity, the measurement of metabolic processes, and the evaluation of cerebral blood flow. The images can be examined in various planes: transaxial (horizontal sections), coronal (vertical sections from anterior to posterior), and sagittal (vertical sections from lateral to lateral), offering thorough insights into brain anatomy [88]. These imaging planes are relevant to all volumetric brain imaging methodologies, facilitating thorough analysis and visualization of the brain's anatomy and functionality from various perspectives. Table 3 summarizes the diverse data types produced by various volumetric brain imaging techniques, their applications, and the imaging planes utilized for brain visualization.

4. Tools and libraries

Progress in neuroimaging has been significantly enhanced by the creation of specialized tools and libraries for processing and analyzing brain imaging data. These tools allow researchers to perform complex analyses, visualize results, and draw significant conclusions from a vast amount of imaging data. Three of the most prevalent tools in the neuroimaging community are FreeSurfer [89] and SPM (Statistical Parametric Mapping) [90].

4.1. *FreeSurfer*

FreeSurfer is software intended for the analysis and visualization of structural and functional neuroimaging data from both cross-sectional and longitudinal studies. It is extensively utilized for processing MRI data, offering tools for cortical surface reconstruction, segmentation of subcortical structures, and the creation of statistical maps. FreeSurfer's primary strengths encompass its proficiency in precise cortical surface reconstruction, which entails segmenting the brain's gray matter and white matter, thereby reconstructing the cortical surface to yield morphometric metrics such as thickness, area, volume, surface area, and curvature. The automated segmentation of subcortical structures, including the hippocampus, amygdala, and basal ganglia, is crucial for volumetric studies examining the size and morphology of these structures across various populations or temporal intervals. FreeSurfer excels at longitudinal analysis, which examines how brain structure changes over time. This feature is especially beneficial for the study of NDDs, as it can offer valuable insights into the mechanisms of the disease and the effects of treatment by monitoring the progression of brain atrophy. The software comprises tools for the alignment of images from various time periods, the correction of motion and other artifacts, and the execution of statistical analyses to identify substantial changes. Besides structural analysis, FreeSurfer facilitates the examination of fMRI data, enabling researchers to project brain activity onto the cortical surface and

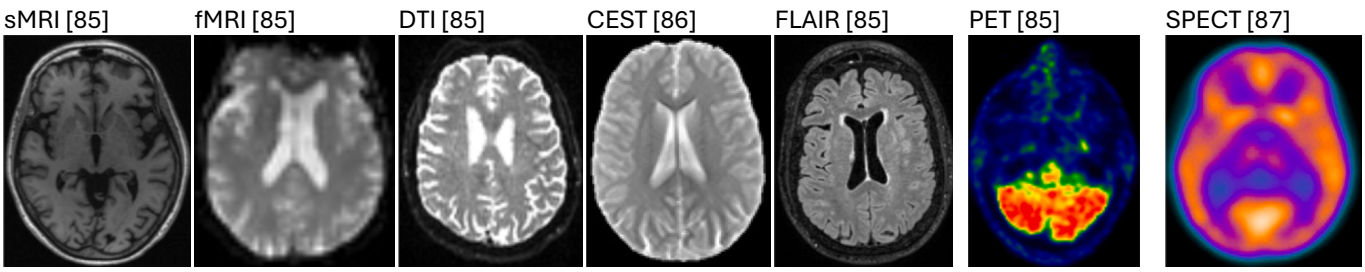

Fig. 1. Brain images obtained from the modalities listed in Table 2: sMRI, fMRI, DTI, CEST, FLAIR, PET, and SPECT. These imaging techniques capture structural, functional, and molecular features of the brain, each offering distinct diagnostic or research value [85–87].

Table 3
Summary of various volumetric brain imaging techniques, their data types, applications, and the imaging planes used to visualize the brain.

Imaging Technique	Data Type	Usage	File Formats
MRI	High-resolution 3D anatomical images	Visualizing brain structure, detecting abnormalities.	DICOM, NIfTI
fMRI	Time-series blood oxygenation data	Mapping brain activity during tasks or at rest	DICOM, NIfTI
DTI	Diffusion-weighted images, tensor maps	Studying white matter tracts and brain connectivity.	DICOM, NIfTI
CEST MRI	Chemical exchange-dependent contrast images	Provides cellular and molecular information about tissue environments, useful in detecting disease-related changes without contrast agents.	DICOM, may vary
FLAIR MRI	Fluid-attenuated inversion recovery images	Enhances contrast by suppressing fluid signals to better identify lesions, particularly in diagnosis of multiple sclerosis.	DICOM, NIfTI
PET	Volumetric tracer concentration images	Measuring metabolic processes, blood flow	DICOM
SPECT	Volumetric gamma radiation images	Assessing cerebral blood flow, neurotransmitter activity.	DICOM

produce statistical maps. Two essential preprocessing steps are image registration and skull stripping, which guarantee precise brain segmentation and surface reconstruction.

4.2. Statistical Parametric Mapping (SPM)

SPM is a Matlab-based software package for analyzing brain imaging data sequences, specifically functional data such as PET, fMRI, and SPECT. Its preprocessing functions, such as realignment, spatial normalization, segmentation, and smoothing, are critical for preparing imaging data for statistical analysis. Multiple templates, such as the default MNI template, can be used for spatial normalization, which registers images to a common space. SPM is well-known for its robust statistical analysis capabilities, which allow researchers to identify regions of the brain activated during specific tasks or conditions. It allows for the examination of particular hypotheses and complex analyses by supporting various statistical models, one of which is the General Linear Model (GLM). SPM provides robust visualization features, enabling researchers to create and exhibit statistical maps that emphasize notable brain activity or variations between conditions. Its intuitive interface and extensive documentation render it accessible to both novice and seasoned researchers. SPM has been employed in numerous studies to examine a range of subjects, from fundamental neuroscience to clinical research.

4.2.1. Computational Anatomy Toolbox (CAT)

CAT is a prevalent extension for sMRI that facilitates the automated processing and analysis of sMRI data. It is utilized in research examining neurological and psychiatric disorders such as Alzheimer's disease, schizophrenia, and major depressive disorder. The capability of CAT to identify subtle morphological alterations in the brain renders it instrumental in comprehending the structural associations of these disorders and in pinpointing potential biomarkers for diagnosis and treatment. VBM, a neuroimaging analysis method, entails the comparison of local concentrations of gray and white matter, facilitating the detection and quantification of structural differences in the brain across various groups. CAT encompasses tools for surface-based morphometry (SBM), facilitating comprehensive analysis of cortical thickness, surface area, and gyrification. The amalgamation of VBM and SBM within CAT permits researchers to perform comprehensive and multifaceted analyses of structural MRI data. The toolbox facilitates sophisticated preprocessing procedures, including bias correction, tissue segmentation, and spatial normalization, thereby enhancing the precision and dependability of ensuing analyses. The CAT automated pipeline streamlines the processing of extensive datasets, rendering it accessible to researchers with diverse levels of proficiency in neuroimaging. It additionally executes image registration to align cerebral images with standardized templates and conducts skull stripping to eliminate non-cerebral tissues from MRI images.

5. Datasets

The learning process in deep learning entails the automatic acquisition of hierarchical features and representations by training a model on a large dataset. This process typically employs neural networks with multiple layers, which is why it is referred to as "deep" learning. This enables the model to capture intricate patterns and structures in the data. Such a database may be too expensive or inconvenient to implement in medical applications in certain cases. Nevertheless, there are public datasets accessible in various domains that can be utilized as training data.

5.1. AD dataset

The Alzheimer's Disease Neuroimaging Initiative (ADNI) [85] offers a comprehensive free open-access longitudinal database for studying AD progression, early detection, and the relationship between structural changes and cognitive declie. It is a multimodal dataset with T1, T2, FLAIR, and diffusion weighted MRI acquisitions, PET scans (amyloid and tau imaging), genetic data (APOE genotyping), CSF biomarkers, cognitive assessments, behavioral assessments, demographic, and health history on individuals with varying degrees of cognitive impairment as well as control subjects. Raw images are available for download in DICOM format and assessment data in CSV separated spreadsheets.

<EXPAND ADNI: Various sub-sets like ADNI 1, ADNI GO, etc. Discuss how acquisition parameters vary across sub-sets, so that is important to take into account when using images and data for training. Have access to the raw images as well as the resulting data from previously preformed image quantifications>.

The National Alzheimer's Coordinating Center (NACC) [91] provides clinical, cognitive, genetic, and imaging data (MRI and PET) from AD Research Centers across the U.S. This dataset is essential for studying brain atrophy, subtle early-stage structural changes, and functional changes in energy utilization linked to amyloid and tau proteins.

Open Access Series of Imaging Studies (OASIS) [92] features free access to T1-, T2-weighted, and FLAIR MRI scans. These scans are crucial for evaluating brain morphology, identifying lesions, and analyzing structural changes linked to aging and NDDs over time.

The Australian Imaging, Biomarkers & Lifestyle Flagship Study of Ageing (AIBL) [93] is a longitudinal study that concentrates on the influence of aging and AD on cognitive function. It encompasses a comprehensive array of data, including amyloid PET imaging, MRI scans, lifestyle data, and health questionnaires, which offer a comprehensive understanding of the progression of AD.

The Japanese Alzheimer's Disease Neuroimaging Initiative (J-ADNI) [94] collects multimodal data, including structural MRI, PET, CSF biomarkers, and genotyping. This dataset emphasizes early-stage AD changes and supports clinical trials by offering surrogate biomarkers for disease-modifying therapies.

International Consortium for Brain Mapping (ICBM) [152] is a global dataset for creating a probabilistic brain atlas with data from diverse demographics. It includes T1-, T2-, and proton density-weighted MRI scans and genetic data, making it valuable for studying brain structure variability across populations.

AddNeuroMed/ANMerge [95,96] Multimodal datasets concentrating on the identification of biomarkers, utilizing T1-weighted MRI alongside processed data including brain volumes and cortical thickness. They facilitate the monitoring of structural alterations over shorter periods, improving early disease identification.

5.2. FTD Datasets

The Frontotemporal Lobar Degeneration Neuroimaging Initiative (FTLDNI) [97] is a longitudinal study utilizing imaging techniques (MRI, FDG-PET), biomarker data, and clinical evaluations to identify brain regions impacted by FTLD. It examines alterations in metabolism, perfusion, and structural integrity to monitor disease progression.

The Genetic FTD Initiative (GENFI) [98] concentrates on genetic FTD, gathering comprehensive neuroimaging, cognitive, and genotypic data from both symptomatic and asymptomatic carriers of genetic mutations such as C9orf72, MAPT, and GRN. It facilitates the identification of biomarkers for early diagnosis and comprehension of disease variability.

5.3. LBD Datasets

LBD data is integrated into broader datasets like ADNI, NACC, and PPMI [99]. These provide volumetric imaging resources and clinical data to study LBD-specific characteristics, such as visual hallucinations and cognitive fluctuations, and to differentiate it from other dementias.

5.4. PD Datasets

The Parkinson's Progression Marker Initiative (PPMI) [99] is a comprehensive dataset featuring clinical assessments, MRI, DTI, PET imaging (dopamine transporter and glucose metabolism), and biospecimens (CSF, blood). It tracks motor and non-motor symptoms, focusing on biomarker validation and understanding PD progression.

5.5. HD Datasets

The PREDICT-HD Huntington Disease Study [100] tracks early biomarkers using longitudinal imaging (T1-weighted MRI, FDG PET) and clinical data to study disease progression before motor symptom onset. The dataset includes processed MRI features like cortical segmentations and gray matter concentrations.

The Track-HD study [101,102] collect longitudinal neuroimaging and cognitive data from premanifest and early-stage HD patients. Advanced imaging techniques, including DTI and fMRI, are employed to investigate compensatory mechanisms and monitor structural and functional alterations in the brain over time.

The IMAGE-HD study [103] examines structural alterations in the neostriatum, particularly the caudate nucleus and putamen. The dataset comprises 3T MRI scans alongside motor, cognitive, and psychiatric evaluations, allowing researchers to associate structural alterations with functional results.

5.6. ALS Datasets

Canadian ALS Neuroimaging Consortium (CALSNIC) is a [104] multicenter platform collecting standardized MRI (T1, T2, DTI, rs-fMRI) and biospecimen data to develop biomarkers for ALS progression. It includes longitudinal data at regular intervals, allowing researchers to analyze structural, functional, and metabolic changes in the brain.

5.7. MS Dataset

The Multiple Sclerosis Segmentation Challenges (MSSC) [105] offers MRI datasets featuring lesion annotations, encompassing T1-weighted and FLAIR images, for purposes such as lesion segmentation and the diagnosis of multiple sclerosis. This data is specifically designed for the development of machine learning models in MS research.

The Hugging Face MS Dataset provides pre-processed multimodal MRI scans accompanied by lesion masks, facilitating seamless integration into workflows. This dataset facilitates automatic lesion segmentation and the classification of multiple sclerosis patients in comparison to healthy controls.

6. Data collection, analysis, and management

6.1. Data collection and analysis

Medical imaging modalities such as MRI and PET scans produce intricate, three-dimensional representations of the brain, facilitating sophisticated analyses of neurodegenerative disorders. Imaging data can be analyzed using two principal approaches, each offering distinct insights into neurodegenerative disease-related structural and functional alterations: cross-sectional and longitudinal analysis.

6.1.1. Cross-sectional analysis

Cross-sectional analysis provides a "snapshot" of brain structure and function at a specific point in time across a diverse sample population. This method enables the comparison of healthy controls with individuals who have NDDs, such as AD. Cross-sectional studies provide essential diagnostic markers by identifying patterns of structural and functional deviations, which help pinpoint brain regions most affected by various NDDs. Hippocampal volume, for instance, can be compared between groups to identify early indicators of degeneration associated with the advancement of AD. Thus, baseline markers that differentiate people with NDD from the general population can be found in cross-sectional data, indicating possible areas of interest for disease detection models.

6.1.2. Longitudinal Analysis

Unlike cross-sectional studies, longitudinal analysis emphasizes monitoring changes within the same subjects across multiple time intervals. This method is essential for monitoring the evolution of neurodegenerative diseases, as it facilitates the detection of temporal alterations that define disease progression. Longitudinal data is especially significant in neurodegeneration research, as the rate of structural alterations (such as hippocampal atrophy in AD) can act as an indicator

for the future severity of cognitive decline. Longitudinal analysis enhances the comprehension of disease progression by documenting temporal changes and augments the predictive accuracy of diagnostic models.

6.1.3. Integrating cross-sectional and longitudinal data

The integration of cross-sectional and longitudinal analyses within deep learning models strengthens the reliability of diagnostic systems. Cross-sectional data can identify structural markers that differentiate healthy from diseased states, whereas longitudinal data facilitates the monitoring of progression rates and the prediction of future disease outcomes. This integration offers extensive insight into the present and future effects of NDDs on brain structure, allowing models to classify disease states and predict disease trajectories.

6.2. Input data management

Deep models have become the prominent approach in a variety of medical image analysis applications. Different types of data, like MRI and PET scans, can be used to train a deep model for the automated analysis of NDDs. These image data contain different types of NDDs-related information that can help with diagnosis prediction [106].

Moreover. These images are inherently 3D because they depict volumetric representations of the brain [107]. Each volume comprises a sequence of 2D slices, which are cross-sectional images acquired along various planes. These slices offer comprehensive spatial data regarding the brain's architecture and functionality, which can be utilized to examine the advancement of neurodegenerative disease-related alterations in the brain. Two-dimensional slices are images captured at designated intervals along a plane within the three-dimensional volume of the brain. Each slice illustrates a "section" of the brain at a specific depth or angle, analogous to how a slice of bread represents a thin segment of an entire loaf. In medical imaging like MRI or PET scans, these slices are taken at regular intervals, either horizontally, vertically, or diagonally, and when combined, they form a complete 3D representation of the brain.

The entire neuroimaging modality remains challenging to manage. Based on the type of feature extraction, in general there are four main approaches to input data management: voxel-based, slice-based, patch-based, and ROI-based [108,109]. (see Fig. **Figure 2** for an illustration of these approaches).

- **Voxel-based Approach**: Voxel-based methodologies utilize the intensity values of each voxel in a volumetric brain scan, facilitating the examination of the entire brain volume. These methods provide a holistic view, encompassing the complete spatial data from the scan. Nonetheless, voxel-based methodologies are hindered by the challenge of managing extensive data volumes, resulting in significant

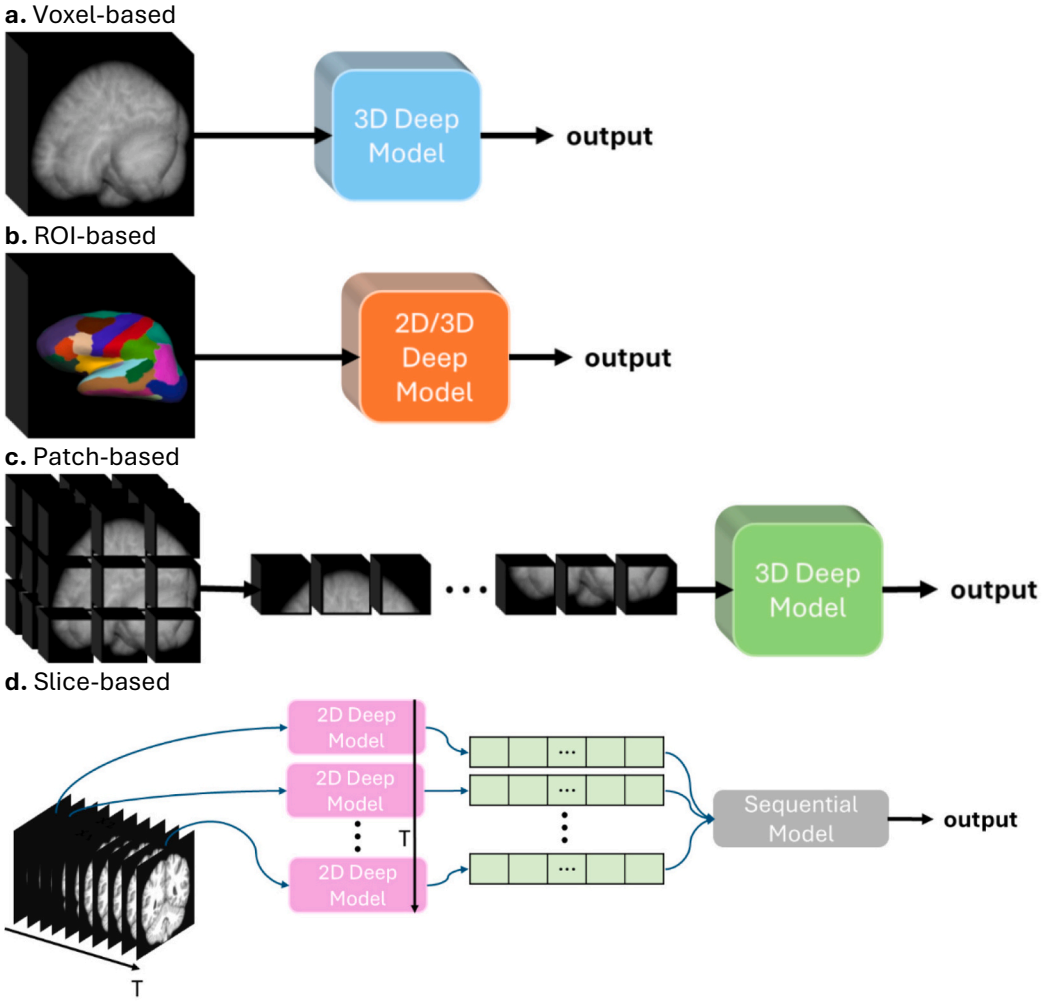

Fig. 2. Illustration of deep learning approaches in volumetric brain imaging: (1) Voxel-based method utilizing the entire brain volume as input to a 3D deep model, (2) ROI-based method focusing on specific regions of interest processed by a 3D deep model, (3) Patch-based method dividing the brain volume into smaller patches for sequential input to a 3D deep model, and (4) Slice-based method analyzing 2D slices of the 3D volume through 2D deep models, followed by a sequential model for temporal or spatial aggregation.

computational requirements. Moreover, analyzing each voxel in isolation may lead to the omission of critical contextual information among adjacent voxels, which could be vital for the precise identification of disease-related alterations [110–116].

- **ROI-based Approach**: The region-of-interest (ROI) methodology focuses on particular brain regions recognized as impacted by NDDs. This approach leverages existing knowledge regarding the brain regions commonly implicated in conditions such as Alzheimer's disease, including the hippocampus. This approach simplifies the data by concentrating on these regions, enhancing its interpretability for clinical application. Nonetheless, ROI-based methodologies may overlook anomalies in regions beyond the designated areas, thereby constraining their capacity to encompass the complete scope of the disease. Moreover, concentrating on larger regions may neglect smaller yet significant anomalies [117–123].
- **Patch-based Approach**: This method involves analyzing smaller segments or patches of the brain image instead of the complete scan. This localized emphasis facilitates the identification of specific regions that may exhibit early indications of disease, even when those regions are minor or nuanced. The difficulty with this method is in identifying the most informative patches to guarantee that the model can discern patterns pertinent to the disease. Incorrectly selected patches may result in the omission of vital information, consequently diminishing model accuracy. Nevertheless, patch-based methods are advantageous due to their sensitivity to localized anomalies [107,124–127].
- **Slice-based Approach**: Slice-based techniques streamline volumetric brain imaging data by partitioning it into two-dimensional slices, facilitating computational processing and management. These slices can be obtained from various planes, such as axial or sagittal, with axial being the most frequently utilized. This method decreases the parameter count but frequently neglects the spatial relationships between adjacent slices, which may be essential for comprehending the progression of diseases such as Alzheimer's. Consequently, while computationally efficient, it may not consistently yield a comprehensive understanding of brain pathology [128–131]

Voxel-based techniques offer intricate detail but are computationally demanding and susceptible to overfitting because of their high dimensionality. Patch-based methodologies diminish computational expenses yet encounter constraints in representing inter-patch relationships, which may lead to the omission of global context. ROI-based methodologies concentrate on clinically pertinent areas, enhancing interpretability and efficiency; however, they may introduce bias and result in information loss beyond the specific regions. Slice-based methods exhibit computational efficiency and utilize 2D models; however, they compromise 3D spatial relationships unless supplementary sequential models are integrated.

7. Deep learning models

Artificial intelligence (AI) comprises a wide array of technologies that allow machines to execute tasks generally necessitating human intelligence [132]. Machine learning (ML) has emerged as a subset of artificial intelligence (AI) dedicated to creating algorithms that enable computers to learn from data and make predictions or decisions accordingly. Machine learning models enhance their performance as the volume of available data for training increases, without explicit programming for specific tasks [133]. DL is a specialized subset of machine learning that utilizes artificial neural networks with multiple layers to model intricate patterns in data. In contrast to conventional machine learning, which necessitates considerable effort and expertise for feature engineering to identify and refine input data features, DL automates this procedure. [134]. In the field of neuroimaging for neurodegenerative diseases, DL methodologies are especially effective due to their proficiency in managing extensive imaging datasets. These models can autonomously identify complex patterns and anomalies in brain scans that frequently signify diseases such as Alzheimer's, Parkinson's, and multiple sclerosis. DL facilitates a more scalable and sophisticated analysis of high-dimensional data by circumventing the manual feature engineering process, significantly surpassing the efficacy of conventional imaging methods. This automation improves the efficiency and scalability of data analysis while potentially revealing new patterns and biomarkers that may be overlooked by human-designed features. Consequently, DL emerges as an essential instrument in research and clinical diagnostics for evaluating and tracking neurodegenerative disorders, providing insights that are both profound and attainable at a speed commensurate with the swiftly increasing data volumes.

The architecture of a DL model is chosen based on the nature of the data and the specific clinical question. In neuroimaging for NDDs, key architectural choices include 2D vs. 3D models and the underlying network type (e.g., CNN, ViT, RNN). in other words, those that analyze images slice by slice (2D slice-based models) and those that process the full 3D brain volume (volumetric models). Volumetric models analyze the complete 3D architecture of neuroimages, enabling the model to discern complex spatial patterns in three dimensions [135]. Three-dimensional models preserve complete spatial relationships within the brain, offering a more comprehensive perspective of its structure. These models are especially beneficial for applications necessitating intricate spatial context, such as the identification of complex neurodegeneration patterns. The 2D slice-based methodology streamlines processing by segmenting volumetric neuroimaging data into 2D slices along anatomical planes (sagittal, axial, and coronal), thereby facilitating the application of established 2D image processing techniques. These methodologies primarily choose the central slices from various planes or determine the most informative slices according to specific criteria. In Hearin, a notable challenge emerges from the loss of inter-slice spatial relationships. Each slice is analyzed independently, resulting in the potential oversight of significant patterns that extend across multiple slices. This may impede the model's capacity to discern the 3D structural information of the brain, which is essential for recognizing intricate neurodegenerative patterns. Multiple solutions have been proposed to resolve this issue. One method is to integrate 2D models with sequential models, such as recurrent neural networks (RNNs) [136,137] or transformer-based time-series networks [138,139], which can capture dependencies between sequential slices [142,143]. Sequential models preserve spatial continuity across the brain by processing the 2D slices in order and allowing the model to learn how features from adjacent slices relate to each other. The utilization of a multi-view approach, which combines slices from various planes to provide complementary information, is another potential solution. This approach has the potential to capture more holistic patterns and compensate for the limitations of analyzing each slice independently.

One of the main advantages of using 2D models in neuroimaging, particularly the slice-based approach, is the ability to draw on pre-trained models from other domains, such as natural image classification. Transfer learning can be used to fine-tune well-known 2D image processing models such as ResNet [140], VGG [141], and EfficientNet [142] for medical applications. This is particularly useful in volumetric medical imaging, where volumetric data may be limited. While 3D models require a large amount of volumetric data for training, which is often limited, 2D models can achieve good performance with fewer data points, making them highly useful in medical scenarios were acquiring and annotating large datasets is challenging. However, when training a model from scratch, 3D models can outperform 2D models in neuroimaging tasks. Because 3D models analyze the entire volumetric structure of the brain in a single pass, they preserve spatial relationships across all dimensions, capturing both local and global patterns that may be important for diagnosis.

Building on these methods, recent research has suggested treating the entire 3D MRI volume as an ordered sequence of slices, enabling

models to capture both slice-level features and the spatial continuity across the entire brain. Transformer-based architectures employing spatiotemporal attention, such as AlzFormer [143], directly analyze the entire MRI volume, capturing global inter-slice relationships in a singular forward pass. This design enhances data efficiency and allows the network to concentrate on clinically relevant brain regions by utilizing interpretable attention maps, which are derived from large-scale vision or video models utilizing transfer learning. Such whole-volume sequence modeling represents a step forward from conventional slice-by-slice analysis because it preserves inter-slice context and captures distributed patterns of neurodegeneration that may span multiple regions. Nevertheless, when very large training datasets are available, fully 3D convolutional models can still offer strong performance by jointly learning local and global features in all three spatial dimensions. Because these models process the entire brain volume as a 3D object, they inherently preserve spatial relationships and can detect subtle structural alterations critical for early disease diagnosis.

Diverse DL models are specifically engineered for image analysis tasks and are extensively utilized for examining neurodegenerative diseases via neuroimaging. These methodologies can be classified into Convolutional Neural Networks (CNNs) [144], Vision Transformers (ViTs) [145], and sequential models such as RNNs and transformer-based time-series networks.

CNNs are exceptionally proficient in the analysis of NDDs owing to their multilayered hierarchical architecture, which is adept at segmentation, classification, and detection tasks. The architecture typically includes convolution, pooling, batch normalization, dropout, fully connected layers, activation functions, and SoftMax layers. CNNs' strong capabilities in image classification make them well-suited for NDDs diagnosis.

ViTs are gaining recognition for their efficacy in the analysis of NDDs. In contrast to CNNs, which utilize convolutions to capture local spatial hierarchies, ViTs employ self-attention mechanisms to model long-range dependencies among image patches, thereby facilitating the capture of global relationships within the data. This renders them especially advantageous for intricate neuroimaging endeavors where comprehending overarching patterns throughout the brain is essential. Nonetheless, while conventional ViTs emphasize global information, several ViT variants, including Swin Transformer [149] and hybrid models that integrate convolutional layers with transformers, have been created to also capture local features. These variants incorporate mechanisms such as local window attention, enabling the models to manage both intricate, local patterns and broader, global context. By integrating the strengths of CNNs in local information acquisition with the robust global attention mechanisms of transformers, these ViT variants exhibit exceptional versatility for NDD diagnosis. They can detect both localized anomalies and extensive structural alterations, offering a thorough methodology for analyzing neuroimaging data in the detection and classification of neurodegenerative diseases.

The training of a DL model is an iterative optimization process designed to reduce the discrepancy between the model's predictions and the actual ground-truth labels. The procedure commences with the specification of a loss function (e.g., cross-entropy for classification tasks), which measures the model's error. Predictions are generated by feeding a collection of data through the network in a forward pass during each training iteration. The calculated loss is then used in a backward pass, an algorithm known as backpropagation, to compute the gradient of the loss with respect to each model parameter (or weight).

An optimizer, like Adam or Stochastic Gradient Descent (SGD), employs these gradients to modify the model's weights, progressively changing them towards minimizing the loss. This fundamental update rule can be expressed as $W_{\text{new}} = W_{\text{old}} - \eta \nabla L$, where W represents the weights, η is the learning rate (a hyperparameter controlling the step size), and ∇L is the gradient of the loss. The model's performance on a distinct validation dataset converges, indicating that it has learned to generalize from the training data, after this cycle of forward pass, loss computation, backpropagation, and weight update is repeated for many epochs (full passes over the entire training dataset).

Hyperparameter tuning is an important step in optimizing any DL model. While some parameters, such as learning rate and batch size, are universal, their optimal values and effects vary significantly between architectures, as shown in Table 4. Aside from these general settings, each model family has a distinct set of structural hyperparameters that must be configured. For example, the kernel sizes and filter count of a CNN have a significant impact on its performance, whereas the patch size and number of attention heads of a ViT govern its behavior. Table 5 summarizes the key architecture-specific hyperparameters.

Table 4
General Hyperparameter Tuning Across Architectures. This table compares the role and typical tuning considerations for fundamental hyperparameters like learning rate, batch size, and optimizers for CNNs, ViTs, and RNNs.

Hyperparameter	CNNs	ViTs	RNNs
Learning Rate	Crucial. Determines the step size during optimization. Often tuned using a scheduler (e.g., ReduceLROnPlateau). Typical range: 1e-5 to 1e-2.	Very sensitive. Often requires a smaller learning rate and a warm-up schedule to prevent instability during early training stages.	Important. A high learning rate can cause gradients to explode, while a low one can lead to slow convergence. Gradient clipping is often used.
Batch Size	Affects training speed and gradient stability. Larger batches provide more stable gradients but require more memory. Common sizes: 32, 64, 128.	Memory intensive. ViTs are large, so batch sizes are often limited by GPU memory. Affects training stability and speed.	Controls how many sequences are processed in parallel. Smaller batches are common due to varying sequence lengths and memory constraints.
Optimizer	Adam is the most common and robust choice. SGD with momentum is also frequently used.	AdamW is standard. It decouples weight decay from the gradient update, which improves generalization for Transformers.	Adam and RMSprop are popular choices as they are effective at handling the unstable gradients common in RNNs.
Dropout Rate	Applied to fully connected layers or sometimes between convolutional layers to prevent overfitting by randomly zeroing out neurons.	Applied within the attention blocks and feed-forward networks. It is a key regularizer for the large ViT models.	Applied to the inputs/outputs of recurrent layers (but not on the recurrent connections themselves) to prevent overfitting on sequential data.
Weight Decay	A common regularization technique (L2 regularization) that penalizes large weights to improve generalization. A small value like 1e-4 is typical.	Essential. ViTs are prone to overfitting, so a stronger weight decay is often necessary compared to CNNs. AdamW is the preferred optimizer for this.	Used to prevent overfitting, though less common than dropout. Careful tuning is needed to avoid hindering the learning of long-term dependencies.

Table 5
Architecture-Specific Hyperparameters. This table details the hyperparameters that are unique to the internal structure of CNNs, ViTs, and RNNs, such as kernel size, attention heads, and hidden units, respectively.

Hyperparameter	Convolutional Neural Networks (CNNs)	ViTs	RNNs
Kernel/Filter Size	Defines the dimensions of the sliding convolution window (e.g., 3x3, 5x5). Smaller kernels capture fine-grained local features.	N/A	N/A
Number of Filters	Determines the depth of the output feature map. More filters allow the model to learn a greater number of features at each layer.	N/A	N/A
Patch Size	The input image is split into fixed-size patches (e.g., 16x16). Smaller patches increase sequence length and computational cost but can capture finer detail.	N/A	N/A
Embedding Dim (D)	The size of the vector representing each image patch. A larger dimension allows for more expressive representations but increases model size.	N/A	N/A
# Transformer Layers	The number of stacked Transformer encoder blocks. More layers increase model depth and capacity to learn complex relationships.	N/A	N/A
# Attention Heads	The number of parallel attention mechanisms in each layer. More heads allow the model to jointly attend to information from different representation subspaces.	N/A	N/A
Hidden Units	Defines the dimensionality of the hidden state in a recurrent layer. More units increase the model's memory and capacity.	N/A	N/A
# Recurrent Layers	The number of stacked RNN layers. Stacking layers allows the model to learn higher-level temporal representations.	N/A	N/A
Cell Type	The choice of recurrent unit. LSTM and GRU are standard choices over vanilla RNNs because they better handle long-term dependencies.	N/A	N/A

8. Deep learning in neurodegenerative disease imaging

This section presents various DL models employed for the early diagnosis of NDDs from 2017 to 2025, emphasizing the essential concepts and algorithms in NDD detection. Moreover, we ignore studies that do not maintain inter-slice relationships, including works that extract features from individual slices separately and then feed them consecutively to the classification method without performing true sequential analysis, because this approach treats each slice independently and fails to capture the spatial or temporal dependencies between consecutive slices, which are critical for accurately modeling and diagnosing neurodegenerative diseases. In this study, methodologies are classified into two primary categories: CNNs and ViTs, both of which have been extensively utilized in the early diagnosis of NDDs.

This review paper includes Tables 6-12 which succinctly summarize DL methods applied to NDDs, outlining specific methodologies, data types, approaches, and significant findings from each cited study. This table seeks to furnish readers with a systematic summary of each study's principal contributions to NDDs research, thereby enhancing comprehension of the advancing terrain of neuroimaging and computational methodologies in relation to neurodegenerative diseases. We present a comprehensive account of these studies, explicitly detailing their methodologies and results.

8.1. Alzheimer's disease

Volumetric data has been handled by adapting classic CNN architectures. 3D convolutional layers were added to ResNet in [153] in order to predict the progression of AD. EfficientNet has recently been adapted to volumetric MRI data, as shown in [157], where 5-fold cross-validation was used to refine the model across folds for robust AD classification.

Table 6
A summary of the reviewed studies on AD

Study	Methodology	Data Type	Approach	Objective
[146]	Fusion of 2D and 3D CNNs	CT	Combined spatial and volumetric information **Slice-based + Voxel-based**	Classified into AD, lesion, and normal aging
[147]	3D-DenseNet	sMRI	Dense connectivity for AD and MCI diagnosis **Voxel-based**	AD and MCI diagnosis
[148]	3D CNN with regression models	rs-fMRI	Used spatial maps for CNN input; predicted MMSE scores **Voxel-based**	Classifying AD and healthy controls
[149]	ResNet with 3D convolutional layers	sMRI	The 3D smoothed gray matter maps are fed into ResNet with a series of 3D convolutional units **Voxel-based**	Predicting progression from MCI to AD
[150]	3D shearlet + Pretrained CNNs + custom CNN	sMRI	Custom 1D CNN model transformed the combined shearlet-based descriptors with deep features **Voxel-based**	AD classification (CN, MCI, pMCI, AD)
[151]	ResNet50 with 3D convolutional layers	sMRI	3D and compact ResNet-50 architecture is designed. **Voxel-based**	Predicted MCI to AD conversion.
[152]	3D ResNet50 super-network	sMRI	Temporal information is inferred using Scan Temporal Order loss and Relative Inter-Scan Interval loss **Voxel-based**	Assessed AD progression through longitudinal scans.
[153]	Combined 3D CNN, pre-trained 2D CNN, and Transformer components	sMRI	2D CNN uses pre-trained weights for 2D representation learning, while 3D CNN uses native 3D representation learning. **Voxel-based**	AD classification (CN and AD)
[154]	Stacked Sparse Autoencoder and Brain Connectivity Graph Convolutional Network	rs-fMRI	The functional connectivity of brain ROI was determined using Pearson's correlation coefficient and a network of edge-based graph convolution, presenting a fully connected graph. **ROI-Based**	The classification of cognitive impairments includes CN, Significant Memory Concern, Early MCI, MCI, Late MCI, and AD.
[155]	3D Jacobian domain convolutional neural network	sMRI	Jacobian determinant maps are used to measure voxel-level volumetric transitions associated with AD. **Voxel-based**	AD classification (CN and AD)
[156]	Combination of VGG-16 and Transformer	sMRI	VGG-16 extracts spatial features from each 2D slice. The sliding-window attention	Tracking of disease progression.

(*continued on next page*)

Table 6 (*continued*)

Study	Methodology	Data Type	Approach	Objective
			mechanism fuses adjacent slice features, capturing long-range spatial dependencies. Temporal attention further models feature evolution across multiple MRIs over time. **Slice-based**	
[157]	EfficietNet-b0 with 3D convolutional layers	sMRI	Processed full volumetric structure using End-to-end learning **Voxel-based**	AD classification (CN and AD)
[158]	Spatial transformer encoder and Temporal transformer encoder	rs-fMRI	Handled temporal dynamics; captured brain region relationships using spatiotemporal graph transformer **ROI-Based**	Categorized data into AD progression stages. AD vs. normal control, early mild cognitive impairment vs. late mild cognitive impairment.
[159]	3D DenseNet121 with transformers	sMRI	Paired current and prior MRI scans; Combined spatial and longitudinal information. **Voxel-based**	AD classification (CN and AD)
[160]	Alzh-Net Upper and Lower	MRI	Utilized dual CNNs for multi-scale feature extraction and interpretation -	AD classification (CN vs MCIc vs MCInc vs AD)

Table 7
A summary of the reviewed studies on FTD

Study	Methodology	Data Type	Approach	Key Findings
[161]	Logistic regression, MLP, 3D-CNN, ViT, MLP-Mixers, gMLP	sMRI	Used whole-brain, frontotemporal masking, ROI analysis **ROI-Based**	Enabled region-specific analysis for bvFTD classification
[162]	Swin Transformer	Diffusion MRI	Applied hierarchical self-attention, window shifting for feature extraction **Voxel-based**	Early diagnosis of FTD
[163]	Deep Grading system with 125 3D U-Nets	sMRI	Produced 3D disease-specific grading maps combined with SVM-based structure analysis **Patch-based**	Multi-disease classification of AD, FTD and healthy controls.
[164]	DenseNet adapted for 3D input	sMRI	**Voxel-based**	Multi-disease classification of AD, FTD and healthy controls.
[165]	VGG16 with 3D CNN	[^{18}F]-FDG PET	**Voxel-based**	Classified MRIs into AD, FTD, and CN

The amalgamation of 2D and 3D CNNs has been investigated to utilize both spatial and volumetric data. A hybrid framework was developed in [146], for the classification of CT brain images into

Table 8
A summary of the reviewed studies on DLB

Study	Methodology	Data Type	Approach	Key Findings
[166]	2D-CNN	SPECT	The 2D-CNN was trained on brain surface perfusion images obtained through three-dimensional stereotactic surface projection. **ROI-Based**	classification for the diagnoses of DLB and AD.
[167]	3D-CNN based on VGG16	[18F]-FDG PET	The model considers the input as a sequence of 2D images obtained along the axial plane from 18F-FDG PET scans **Voxel-based**	Discriminating between the diagnoses of AD, MCI-AD, DLB, and CN

categories of AD, lesions (such as tumors), and normal aging. The 2D CNN examined axial slices, whereas the 3D CNN evaluated segmented 3D blocks, with the ultimate classification dependent on the average of SoftMax scores.

Advanced Architectures for Volumetric Data have effectively employed DenseNet-based models for the analysis of volumetric data. In study [147], 3D-DenseNet with dense connectivity was implemented on MRI scans to facilitate feature reuse and improved gradient flow, thereby facilitating the diagnosis of AD and MCI. Building on this, study [159] used DenseNet121 with paired MRI scans to combine spatial and temporal features for longitudinal analysis, allowing detailed tracking of changes over time in neurodegenerative conditions.

Transformers have been progressively incorporated into AD diagnostic workflows. In [153], multi-plane and multi-slice transformer networks were employed in conjunction with CNNs for global pattern recognition across MRI planes. Furthermore, [158] presented a spatio-temporal graph transformer for the analysis of volumetric rs-fMRI data, employing temporal and spatial transformer encoders to model variations in activity and inter-regional interactions. Furthermore, recent research has broadened the application of transformers to time-series imaging. A pre-trained ViT was utilized in [139],for feature extraction from MRI slices, subsequently employing time-series modeling to elucidate inter-slice relationships for AD classification.

Pretrained models and transfer learning methodologies have enabled effective feature extraction for AD diagnosis. In [150], retrained CNNs extracted slice-level features that were amalgamated into a singular representation for MRI classification. Likewise, [151] employed transfer learning to refine a 3D CNN originally trained on normal control and AD scans, modifying it to forecast the transition from mild cognitive impairment to AD.

Resting-state functional MRI (rs-fMRI) data have been utilized to detect alterations in brain connectivity. In [148], a 3D CNN categorized AD utilizing spatial maps obtained from resting-state fMRI scans, whereas conventional regression models forecasted Mini-Mental State Examination (MMSE) scores. In [154], stacked sparse autoencoders (SSAE) were utilized on rs-fMRI data to model sparse brain activity patterns and connectivity signatures for AD classification.

Explorations of innovative input representations have been conducted to improve classification. Jacobian determinant maps were generated from affine-registered MRI images in [155], emphasizing voxel-level tissue alterations associated with AD. These maps facilitated a 3D CNN in recognizing structural degeneration patterns linked to AD. Likewise, [156] employed sliding-window attention mechanisms to concentrate on nuanced longitudinal variations in limited sMRI datasets. Finally, Venkat et al.[160] developed an architecture that integrates multiple CNNs, Alzh-Net Upper and Alzh-Net Lower, each designed to

Table 9
A summary of the reviewed studies on PD

Study	Methodology	Data Type	Approach	Key Findings
[168]	PD Net (3D CNN)	FP-CIT SPECT	**Voxel-based**	Identified PD from NC
[169]	ResNet and RNN combined	MRI and DaT scans	ResNet exploits the spatial structure, while RNN exploits the temporal structure **Slice-based**	Identified PD from NC
[170]	ResNet50	Neuromelanin-sensitive MRI	The CNN employs axial slices and transforms them into output vectors with class probabilities through a chain of convolutional layers. **Slice-based**	classification for the diagnoses of PD and atypical parkinsonian syndromes
[171]	3D CNN	DaTscan SPECT and UPDRS scores	The model processes scans from two time points separately using 3D CNNs, flattens them, merges with clinical scores, and predicts disease progression via fully connected layers. **Voxel-based**	Longitudinal clinical measures to track disease progression over time.
[172]	2D and 3D CNNs	MRI	2D model consists of multiple independent 2D slices stacked together, but it lacks spatial connectivity along the third dimension. **Slice-based and Voxel-based**	Identified PD from healthy-controls
[173]	2D CNN	Diffusion MRI	Each slice id processed independently with a 2D CNN, and aggregates predictions for diagnosis without capturing inter-slice relationships. **Slice-based**	Identified PD from NC
[121]	3D CNN	DTI	Segmented brain into ROIs and trained on each **ROI-based**	diagnosing healthy control and idiopathic PD
[174]	Hybrid CNNs (VGG16, DenseNet, LSTM)	MRI and SPECT	using LSTM to maintain inter-slice dependencies **Slice-based**	Identified PD from NC
[175]	Segmentation + DenseNet + traditional classifiers	123I-Ioflupane SPECT and 3 Tesla MRI	Averaging feature maps across slices **ROI-based and Slice-based**	Predict the HoehnYahr stages of PD
[176]	ResNet + traditional classifiers	sMRI and clinical features,	Aggregating features across slices **ROI-based and Slice-based**	Predict whether a PD patient is a "Good Responder" or "Bad Responder" to levodopa treatment.
[177]	3D CNN	Multimodal (sMRI and DTI)	Maintain spatial correspondence across modalities **Voxel-based**	Identified PD from healthy-controls

Table 10
A summary of the reviewed studies on HD

Study	Methodology	Data Type	Approach	Key Findings
[178]	3D-ResNet	sMRI	3D ResNet-50 architecture is designed. **Patch-based**	Classified scans into healthy control, manifest HD, pre-manifest HD
[179]	Pulse-Coupled Neural Network and GoogLeNet fusion	Multi-modal (MRI, SPECT)	The model extracts features from each MRI slice using GoogLeNet. These features are then fused at the slice level using Hahn moments and Pulse-Coupled Neural Network **Slice-based**	Improved diagnostic accuracy through feature fusion
[180]	U-Net-based segmentation model	sMRI	The volumetry process included segmenting structures of interest, calculating volumes from segmentation masks, and comparing these volumes to a reference database of healthy individuals. **Voxel-based**	Automated brain volumetry in HD patients

increase the efficiency of specific feature extraction tasks in MRI classification. This architecture facilitates the extraction of features at multiple levels of abstraction and detail, thereby augmenting the system's capacity to interpret and classify intricate MRI data efficiently.

8.2. *Frontotemporal dementia*

DL has been widely used to classify FTD and its variants, utilizing a variety of architectures and neuroimaging modalities to improve diagnostic accuracy. Several studies have focused on multi-model and region-specific approaches using structural MRI data. Di Benedetto et al. [161] investigated logistic regression, multilayer perceptron (MLP), 3D CNNs, ViTs, MLP-Mixers, and gated MLPs (gMLP) for the classification of behavioral variant frontotemporal dementia (bvFTD) in comparison to healthy controls. Their analysis utilized three preprocessing techniques: whole-brain analysis, frontotemporal masking, and ROI analysis. The ROI methodology specifically focused on clinically pertinent brain regions, including the frontal and temporal lobes, by training sub-models for these areas and amalgamating outputs into a region-specific classification score. Similarly, Nguyen et al. [163] used T1-weighted MRI data to create a multi-disease classification framework for AD and FTD. Their novel deep grading (DG) maps, created with an ensemble of 125 3D U-Nets, revealed disease-specific anatomical patterns. These grading maps were combined with volumetric data from

Table 11
A summary of the reviewed studies on ALS

Study	Methodology	Data Type	Approach	Key Findings
[181]	U-Net encoder-decoder	sMRI	Each slice was processed separately **Slice-based**	Analyze the Visceral Adipose Tissue/ Subcutaneous Adipose Tissue ratio in ALS patients
[182]	ViT and global filter network	T1W, R2*, and FLAIR	The model processes volumetric MRI slice-by-slice, extracting spatial and frequency features from each 2D slice, then fusing them using linear fusion for final classification. **Slice-based**	classifying ALS patients from healthy controls
[183]	DEEPCATCH (DL software)	Abdominal CT scans	2D CNN is applied slice by slice. Then reconstructs volumetric fat and muscle measurements by aggregating segmentations across slices **Slice-based**	prognosis analysis in ALS patients

Table 12
A summary of the reviewed studies on MS

Study	Methodology	Data Type	Approach	Key Findings
[184]	ResNet with 3D layers	T1-weighted and T2-FLAIR MRI	**Voxel-based**	Classified disability levels in MS patients

AssemblyNet segmentation to generate input features for MLP and SVM classifiers, resulting in robust classification.

Transformer-based methods have shown promise in FTD diagnosis, particularly with diffusion MRI data. Tiwari et al. [162] presented a Swin Transformer framework for sparse diffusion MRI, emphasizing the reduction of scan duration and computational complexity. The patch-based architecture segmented diffusion MRI data into non-overlapping patches, utilizing window-based self-attention mechanisms to effectively extract long-range spatial relationships. By shifting windows to create overlapping areas, the model identified intricate spatial correlations. Dense layers utilizing innovative activation functions enhanced diffusion tensor components, facilitating precise estimation of DTI parameters, including Fractional Anisotropy (FA) and Mean Diffusivity (MD), with a reduced number of diffusion directions.

Moguilner et al. [164] used raw T1-weighted MRI data from geographically diverse datasets, including standard 3T and routine clinical 1.5T scans, to develop a DenseNet-based framework for classifying AD, bvFTD, and healthy controls (HC). Their architecture used densely connected convolutional layers to improve feature propagation and reuse while remaining computationally efficient. Data augmentation techniques, such as rotations, flips, and Gaussian noise addition, increased model robustness. Occlusion sensitivity analysis revealed that the hippocampus was critical for AD classification, while the ventral anterior insula was essential for bvFTD classification. Similarly, Rogeau et al. [165] used [18F]-FDG PET data to classify AD, FTD, and CN. Their 3D CNN, modeled after the VGG16 architecture, used convolutional blocks and dense layers to extract spatial features for precise disease classification.

8.3. Lewy body dementia

Iizuka et al. [166] proposed a DL-based imaging classification system to distinguish dementia with DLB from AD and normal cognition (NL) utilizing brain perfusion SPECT images. The methodology utilized a 2D-CNN trained on brain surface perfusion images produced via three-dimensional stereotactic surface projection (3D-SSP). The model concentrated on recognizing the cingulate island sign (CIS), a hallmark of DLB. The CNN comprised convolutional layers succeeded by max-pooling and ReLU activation. The final SoftMax layer was employed for binary classification among the groups (DLB vs. AD, DLB vs. NL, and AD vs. NL). Grad-CAM was utilized to illustrate the areas highlighted by the model during classification, demonstrating the significance of the CIS in differentiating DLB from AD.

Etminani et al. [167] developed a 3D-CNN to categorize brain [18F]-FDG PET scans into four categories: AD, dementia with Lewy bodies, MCI due to AD (MCI-AD), and CN. The model architecture was constructed using VGG16 and included convolutional and pooling layers to extract volumetric features from the PET scans. To prevent overfitting, dropout layers were implemented, and the network's outputs were subjected to a SoftMax activation for final classification.

8.4. Parkinson's disease

DL has transformed PD research, facilitating precise diagnosis and progression forecasting through imaging and clinical data. Key methodologies include slice-based and temporal modeling techniques, which examine 2D cross-sections and sequential dependencies to derive significant features.

A DL framework, PD Net, was created as a 3D CNN model for analyzing FP-CIT SPECT images in PD diagnosis [168]. The model's architecture comprises sequential 3D convolutional layers utilizing ReLU activation and max-pooling, converting input SPECT volumes into feature representations for binary classification as PD or CN. PD Net processes volumetric SPECT images by employing multiple convolutional layers to extract pertinent features, subsequently utilizing fully connected layers and a SoftMax classifier for the final output.

Kollias et al. integrated CNN and RNN architectures to create a comprehensive deep model for diagnosing Parkinson's disease [169]. The model was trained in two stages: from scratch with random initialization, and then with transfer learning, which applied pre-trained ResNet-50 weights to the convolutional and pooling layers. Separate networks processed MRI triplets and DaT scans, and the outputs of both networks were concatenated at the input of the first fully connected layer, allowing for integrated analysis of various imaging modalities in PD classification.

Shinde et al. used deep CNNs on neuromelanin-sensitive MRI data to distinguish PD patients from healthy controls and those with atypical parkinsonian syndromes[170]. The CNN framework used axial slices of the brainstem, specifically around the substantia nigra pars compacta (SNc), a region severely affected by Parkinson's disease. Using a ResNet50-based architecture with residual connections, the CNN extracted complex spatial features across multiple layers, learning relevant PD markers directly from the data. To interpret the learned features, discriminative localization was used, with class activation maps (CAMs) highlighting the regions of the SNc that contributed the most significantly to classification. This method facilitated an understanding of how the CNN model maintains spatial coherence across slices by focusing on disease-specific patterns in critical anatomical regions, rather than relying on single, isolated features.

Using non-imaging clinical data, specifically UPDRS-III scores from baseline and year 1, as well as DaTscan SPECT imaging, a CNN method is developed in to predict motor function scores for PD patients at year 4. This model used multiple 3D convolutional layers to process longitudinal imaging data, allowing it to bypass the manual feature extraction required by other approaches. The CNN predicted motor function

progression by combining data from baseline and follow-up assessments to model longitudinal changes, significantly improving outcome prediction accuracy over methods excluding DaTscan images. [172] proposed two CNN-based methods for categorizing MRI scans for Parkinson's disease diagnosis. The first approach used a 2D CNN to process individual slices independently, whereas the second used a 3D CNN to leverage full MRI volumes, capturing inter-slice spatial relationships that are critical for accurate classification. The 3D CNN model's ability to analyze the entire volumetric structure allows it to better identify Parkinson's features by retaining inter-slice dependencies within the MRI data, making it especially useful for this application.

Yasaka et al. used structural connectome matrices from diffusion MRI data to develop a CNN model for categorizing PD [173] proposed two CNN-based methods for categorizing MRI scans for Parkinson's disease diagnosis. The first approach used a 2D CNN to process individual slices independently, whereas the second used a 3D CNN to leverage full MRI volumes, capturing inter-slice spatial relationships that are critical for accurate classification. The 3D CNN model's ability to analyze the entire volumetric structure allows it to better identify Parkinson's features by retaining inter-slice dependencies within the MRI data, making it especially useful for this application.

Yasaka et al. used structural connectome matrices from diffusion MRI data to develop a CNN model for categorizing PD [121] created a CNN-based method for classifying PD. The brain was divided into 90 ROIs using the Automatic Anatomic Labeling template, and the fractional anisotropy (FA) and mean diffusivity (MD) features were calculated for each ROI. A 3D CNN was trained individually on each ROI to assess its predictive power, and model performance was measured using AUC values for each region. In order to improve classification performance, a greedy algorithm was applied to combine the individual CNN models from different ROIs. The algorithm iteratively selected and stacked regions based on their AUC scores, forming an optimized combination of regions that maximized classification accuracy.

By combining DL models (VGG16, DenseNet, DenseNet-LSTM, and InceptionV3) with MRI (T1, T2-weighted) and SPECT DaTscan datasets, a hybrid method for diagnosing PD was created in [174]. To handle volumetric data and maintain inter-slice relationships, the method applies DenseNet-LSTM, where the LSTM component models sequential dependencies between slices, capturing spatial patterns across the 3D volume. This design allows the model to retain inter-slice connections essential for accurate classification of PD.

Aiming to predict Hoehn-Yahr stages at baseline (year 0) and subsequently after four years, Jiang et al. used a 2D DenseNet to analyze PD using 123I-Ioflupane SPECT images [175]. The DenseNet model analyzed axial 2D slices exhibiting significant uptake in the striatum, generating deep features (DF) for model training and prediction. Furthermore, radiomic features (RaF) that encapsulate intensity and texture data were derived from segmented striatal regions. The research combined deep features and radiomics to examine the inter-slice relationship by averaging feature maps across slices, enabling the model to capture spatial dependencies in volumetric data.

Bae er al. established a method to extract spatial features from T1-weighted MRI images to aid in predicting levodopa response in PD [176]. To handle the volumetric MRI data, a ResNet-based model (MedicalNet) was applied, serving as a feature extractor without further modification, which preserved 3D spatial relationships within the data. Additionally, the extracted features were visualized using GradCAM, which mapped each retained feature to its corresponding brain region. This facilitated the spatial visualization of critical areas that influenced classification. In order to enhance the accuracy of classification, a variety of feature selection methods were implemented to optimize the extracted features. Also, machine learning models (SVM, XgBoost, and MLP) were implemented to classify response types based on the spatial features obtained from MRI.

Camacho et al. employed a 3D CNN to process multimodal MRI data, including T1-weighted and DTI scans, to classify PD patients and healthy controls [177]. The CNN model was trained on six imaging maps that depict both macro- and microstructural brain changes (volumetric differences and DTI metrics such as fractional anisotropy) throughout the brain. The 3D CNN concurrently processed the entire volumetric dataset to preserve inter-slice spatial relationships, enabling the capture of spatial and structural information across neighboring slices. This method maintained the spatial coherence necessary for examining 3D brain structures and recognizing distinctive patterns associated with Parkinson's disease throughout the brain's architecture.

8.5. Huntington's disease

For HD classification tasks, [178] proposed a hybrid approach that uses DL and patch-based grading to identify structural abnormalities in brain MRI scans. The approach uses a library of healthy control (HC) templates to identify local differences in the brain by comparing intensity patches. Specifically, a patch-based abnormality metric (PBA) and a patch-based grading metric (PBG) are used to identify subtle structural changes. For classification, a 3D CNN architecture based on ResNet is used, with 3D patches of brain images as input. To manage GPU memory limitations, the data is divided into non-overlapping 3D patches, which are passed through the network. The study maintains inter-slice relations by focusing on 3D patch representations that capture spatial continuity across slices, enhancing the model's ability to understand the structural coherence within the volumetric data.

To clinical diagnosis of NDDs like HD, [179] developed a framework that combines multi-modal brain images. The method integrates Pulse-Coupled Neural Network (PCNN) and CNN architectures for fusion, aiming to retain important features from each modality while improving overall information content. The PCNN component extracts detailed features from individual modalities, whereas the CNN learns a fused representation based on complementary information from multiple modal inputs. This fused output is then fed into a classification network, which improves diagnostic accuracy by combining the strengths of different imaging types like MRI and CT. The framework is completely automated and end-to-end, making it ideal for clinical settings that require rapid and accurate diagnosis. The framework is fully automated and end-to-end, making it ideal for clinical settings requiring quick and accurate diagnosis.

Haase et al. [180] performed an external assessment of a DL software designed for automated brain volumetry in individuals with Huntington's disease. The study included 11 HD patients with genetically validated diagnoses and imaging-confirmed caudate nucleus atrophy, as well as an 11-person healthy control group that was age and gender matched. MRI data was analyzed retrospectively, employing volumetric T1-weighted sequences acquired with either 1.5T or 3T scanners. The methodology utilized a U-Net-based DL segmentation model for the volumetric assessment of diverse brain structures, such as the caudate nucleus, putamen, globus pallidus, and additional supratentorial regions. The volumetric process involved segmenting relevant structures, computing volumes from segmentation masks, and contrasting these volumes with a reference database of healthy individuals. To assess the software's efficacy, the automated caudate nucleus volumes were juxtaposed with manually segmented volumes utilizing 3D Slicer software. Manual assessments of caudate atrophy were quantified utilizing clinically established ratios, specifically the frontal horn width to intercaudate distance (FH/CC) and the intercaudate distance to inner table width (CCI/IT). The ratios, in conjunction with the automated volumetric data, performed statistical analysis to assess the software's accuracy and its concordance with manual methods.

8.6. Amyotrophic Lateral Sclerosis

Vernikouskaya et al. [181] proposed a DL pipeline utilizing an encoder-decoder U-Net architecture to automate the segmentation and quantification of abdominal adipose tissue compartments, namely

subcutaneous adipose tissue (SAT) and visceral adipose tissue (VAT), from T1-weighted MRI scans. The study's goal was to distinguish the patterns of body fat distribution between the 155 participants—74 ALS patients and 81 healthy controls. In the proposed U-Net model, feature channels were reduced to 16, 32, and 64 channels, respectively, in a contracting path with three down-sampling steps and matching up-sampling layers. For downsampling, the network used max-pooling, and for upsampling, it used transposed convolutions. In the last layer, a SoftMax activation function was used to segment pixels in three classes: background, VAT, and SAT.

The SF2Former [182] framework is a transformer-based DL model designed to classify ALS patients and healthy controls based on volumetric MRI data. The architecture is intended to use both spatial and frequency domain features, combining ViT and Fourier-based frequency analysis to improve classification accuracy. The model employs two main branches for feature extraction: a spatial branch and a frequency branch. The spatial branch employs a ViT to extract long-range spatial dependencies from 2D coronal MRI slices, thereby effectively modeling structural relationships within the brain. The frequency branch, on the other hand, uses the Fourier Transform and GFNet modules to extract complementary frequency-domain features. These frequency-based features are critical for detecting global patterns and periodicity in MRI data that might not be visible in the spatial domain. The features obtained from the spatial and frequency branches are combined utilizing a linear fusion mechanism. This amalgamation integrates the advantages of both fields, yielding a cohesive representation that underpins classification. To ensure robust subject-level predictions, the framework uses a majority voting mechanism. Individual slice-level predictions are aggregated to classify the entire subject as either ALS or health control.

Choi et al. [183] conducted a study investigating the prognostic value of adipopenia and sarcopenia in patients with ALS using DL-based body composition analysis from abdominal CT scans. They examined data from 80 ALS patients gathered retrospectively from a single institution, including total, visceral, and subcutaneous fat volumes, as well as skeletal muscle areas at the L3 level. These data were normalized to create indices like the Fat Volume Index (FVI) and Skeletal Muscle Index (SMI).The research employed DL software (DEEPCATCH) for the volumetric segmentation of CT images, yielding automated assessments of adipose and skeletal muscle compartments. Adipopenia was characterized as the lowest sex-specific quartile of the Fat Volume Index (FVI), whereas sarcopenia was identified using established Skeletal Muscle Index (SMI) cutoff values. Correlations between these body composition parameters and clinical metrics, including BMI, ALS Functional Rating Scale-Revised (ALSFRS-R) scores, and progression rate, were examined. The researchers used multivariable Cox regression models to study the relationship between adipopenia and sarcopenia and overall survival. Adipopenia was recognized as an independent prognostic indicator, with patients displaying diminished FVI values experiencing markedly shorter survival durations. Subgroup analyses indicated that adipopenia significantly influenced survival in patients with advanced disease stages. This study illustrated the efficacy of CT-based body composition analysis as a prognostic instrument in the management of ALS.

8.7. Multiple Sclerosis

Coll et al. [184] developed a 3D-CNN based on a residual architecture to classify disability levels in MS patients using T1-weighted and T2-FLAIR MRI data. The network consisted of four residual blocks for feature extraction, succeeded by a global adaptive pooling layer to diminish dimensionality. To predict disability levels, the final feature vector was subjected to additional convolutional layers and a SoftMax classifier. Disability levels were classified as mild or no disability (EDSS < 3.0) and moderate disability (EDSS ≥ 3.0). The research employed Layer-Wise Relevance Propagation (LRP) to produce attention maps, emphasizing brain regions that influence the model's predictions, such as the frontotemporal cortex, cerebellum, and periventricular white matter.

9. Discussion

This review paper aims to expand the existing research on NDDs by focusing on the latest advancements in neuroimaging techniques and the integration of DL models. It highlights the potential of volumetric neuroimaging modalities and DL algorithms in improving early diagnosis and disease monitoring in the most common NDDs. The review fills in the gaps in the existing research, which has mostly focused on common NDDs like AD and PD, by giving a broad look at a wider range of NDDs, such as ALS, MS, FD, and DLB. The paper also explores the different data types prevalent in brain imaging, highlighting the challenges and methodologies associated with each, especially concerning volumetric brain image data. It offers a comprehensive list of volumetric image datasets that are available for every NDD that is discussed, providing useful resources for further study. The review bridges the gap between conventional data analysis methods and contemporary, automated data handling techniques by cataloguing key tools and libraries for brain image analysis and pre-processing. The paper highlights the potential of DL in volumetric brain imaging and points to future directions for early detection and treatment of neurodegenerative diseases by detailing its applications across various NDDs.

One of the most difficult aspects of analyzing volumetric neuroimages for NDD diagnosis is understanding and effectively modeling the spatial relationships between the slices. While voxel-based approaches preserve all spatial information, they may fail to explicitly model these relationships, making them computationally expensive for capturing holistic, global relationships. Patch-based methods significantly limit the model's ability to identify inter-patch relationships, necessitating meticulous attention to patch size and combination strategies to capture larger-scale patterns, whereas ROI-based approaches may concentrate solely on familiar ROIs, thereby overlooking pertinent information. Slice-based methodologies exhibit constrained capabilities in capturing inter-slice relationships, as they are frequently processed independently, potentially resulting in the loss of information along the slice dimension unless techniques such as RNNs or attention mechanisms are employed.

A primary challenge in the clinical implementation of DL is developing a model that accurately represents real-world data. Recent DL models, particularly those concentrating on diagnostic categorization, have achieved amazing accuracy comparable to that of expert visual assessments [185]. A significant limitation of these models was their challenging applicability to actual patients in clinical settings, as certain disease types and their distinctive patterns of abnormalities were not encompassed within the recognized features of the training cohort.

Many conflicting inferences have been reported in literature, in which findings from small, distinct cohorts are used to generalize conclusions for an entire population, without accounting for inter-scanner, intra- and inter-site variations. A theoretically feasible method involves gathering a comprehensive dataset that adequately encompasses all patient demographics; nevertheless, this may lead to numerous practical challenges, including harmonization, data incompleteness, class imbalance, and substantial expenses [186].

On the other hand, hardware, acquisition settings, reconstruction algorithms, incompatible data formats, and data quality are just a few of the things that can cause variations in large scale data [187]. This variability poses a major challenge because it can lead to inconsistencies in data, which complicates the comparison and combination of findings over time and across different locations. As a result, achieving reliable and comparable analyses becomes difficult, potentially leading to misleading conclusions.

10. Challenges and future directions

The present DL success will lead the way for additional research areas and the enhancement of current models. This section explores into

various obstacles and possible pathways for future research and development, with an emphasis on NDDs applications.

- **Variability and Diversity**

Most DL methods are often trained on data from a single site or geographic area drawn from the same distribution, which can limit their applicability to other sites. In brain imaging, differences in operating conditions such as varying scanner types and imaging protocols at different sites often lead to a significant discrepancy in data distribution. Consequently, applying a model trained with data from one scanner to another, or from one site to another, may result in a performance drop. Therefore, large-scale brain image datasets from multiple sites and scanners have enhanced research on the human brain. There is a lot of interest in pooling data across multiple sites because doing so may increase statistical power by combining datasets from different sites and scanners [188]. However, applying a DL model across different imaging sites or scanners, collecting, labeling, and re-training models for each variation is a necessary but heavy process. Collecting data from multiple sites introduces challenges related to inter-site and inter-scanner variability that all affect data from imaging modalities. Even for a single patient, longitudinal studies that use imaging modalities such as MRI, DTI, PET, and CT face significant challenges due to inter-site and inter-scanner variability. If these divergences are not resolved, neuroimaging studies may have less statistical power, their findings may not be applicable across sites, and it may be more difficult to combine and analyze datasets from multiple sites [189]. Consequently, harmonizing neuroimaging data to reduce inter-site and inter-scanner effects is in demand. A number of large-scale efforts have been proposed to address inter-scanner variability and site effects in neuroimaging. For example, [190] developed an attention-guided deep domain adaptation (ADA) framework for multi-site MRI harmonization and automated brain disorder identification. The framework combines three modules: an MRI feature encoder to extract representations, an attention module to locate discriminative brain regions, and a domain transfer module trained adversarially to align source and target domains. They tested the method on 2572 subjects from four public T1-weighted MRI datasets and showed that it improves classification performance and disease progression prediction while highlighting clinically meaningful brain regions. Moreover, [191] proposed a goal-specific harmonization that incorporates downstream task performance as a regularization term during harmonization. The framework is compatible with DL harmonization models and was implemented with a conditional variational autoencoder (cVAE). Using 10,085 T1-weighted scans from 2,787 participants across three international datasets, the model preserved biological information and improved downstream prediction of MMSE scores and clinical diagnoses while still achieving strong dataset harmonization.

- **Class Imbalance**

Class imbalance in medical datasets affects disease prediction and diagnostic tools in DL and medical diagnostic studies. DL algorithms typically prioritize the majority class and ignore the minority class [192]. DL algorithms bias towards the data's dominant class and ignore outliers because of the dataset's inherent imbalance. The balance in real-world datasets is frequently unattainable, and the ill-prepared DL models are unable to detect rare cases of interest, which is a significant concern in medical research. Learning from imbalanced datasets is a frequent but challenging task for DL models. For instance, [193] proposed an automated DL model with an optimal information fusion framework for brain tumor classification from MRI. To address dataset imbalance, they generated new images using a sparse autoencoder. Two pretrained neural networks were fine-tuned with Bayesian optimization, and deep features were extracted from their global average pooling layers. To remove irrelevant information, they introduced an improved Quantum Theory-based Marine Predator Optimization (QTbMPA) algorithm to select the most discriminative features. The selected features were fused in a serial-based manner and classified using neural network classifiers. Experiments on an augmented Figshare dataset achieved very high performance (accuracy 99.80%, precision 99.83%, sensitivity 99.83%) and ablation studies confirmed the contribution of each component. Additionally, [194] proposed ResRepANet, a 3D Residual RepVGG Attention network designed for ADclassification from MRI. The network uses lightweight residual RepVGG blocks to balance accuracy and computational efficiency. A key innovation is the Non-local Context Spatial Attention (NCSA) block, which aggregates global contextual information to enhance the representation of discriminative brain regions. They also introduced a Gradient Density Multiple-weighting Mechanism (GDMM) to adaptively reweight samples based on gradient norms, reducing the influence of outliers and class imbalance. Experiments on ADNI and AIBL datasets demonstrated superior accuracy, sensitivity, specificity, and AUC compared to state-of-the-art methods. While various strategies exist to address this problem, methods that generate artificial data for the minority class can offer a more general solution compared to direct modifications to algorithms.

- **Labeling and Annotating**

The availability of accurately labeled/annotated NDDs data is a significant obstacle. The rapid growth of publicly available data from large-scale projects is driving progress and transparency in neuroimaging [195]. However, labeling/annotating medical images and records necessitates expert knowledge, and the time-consuming nature of the process limits the amount of annotated data available for training DL models. This scarcity of labeled data can impede the development of models that are both precise and generalizable. In such instances, the objective of DL is to integrate semi-supervised training techniques in order to satisfy the criteria for effective learning [196]. To facilitate the comprehension of patterns in unlabeled/unsupervised data, additional research would incorporate existing labeled/supervised data to optimize data modeling and refine learned patterns and representations.

10.1. Future research recommendations

Future research should focus on developing domain-generalizable models capable of training on multi-site datasets without necessitating site-specific fine-tuning. Moreover, the challenges presented by limited annotated data and class imbalance may be overcome through additional investigation of data-efficient learning paradigms, such as synthetic data generation, semi-supervised learning, and self-supervised learning. Additionally, further exploration of data-efficient learning paradigms — including self-supervised learning, semi-supervised learning, and synthetic data generation — could mitigate the challenges posed by limited annotated data and class imbalance. Benchmarking studies that compare 2D, 3D, and spatiotemporal transformer architectures across standardized datasets would provide exact direction on model selection for NDDs diagnosis. Lastly, future research should focus on interpretability and clinical validation, ensuring that attention maps or feature attribution techniques align with established neuroanatomical biomarkers and are assessed prospectively within actual clinical workflows.

CRediT authorship contribution statement

Taymaz Akan: Writing – review & editing, Writing – original draft, Validation, Methodology, Conceptualization. **Sara Akan:** Writing – review & editing, Writing – original draft. **Sait Alp:** Writing – review & editing, Writing – original draft. **Christina Raye Ledbetter:** Writing – review & editing. **Ahmad P. Tafti:** Writing – review & editing, Validation. **Octavio Arevalo:** Writing – review & editing. **Mohammad Alfrad Nobel Bhuiyan:** Writing – review & editing, Validation, Funding

acquisition, Conceptualization.

Consent for publication

Not applicable. This article does not contain any individual data or identifiable information.

Ethics approval and consent to participate

This study did not involve human participants or animals, and ethics approval was therefore not required.

Funding

This work was supported by an Institutional Development Award (IDeA) from the National Institutes of General Medical Sciences NIH under grant number P20GM121307 to MANB. This project is also partially supported by Ike Muslow, MD, Endowed Chair in Healthcare Informatics of LSU Health Sciences Center Shreveport.

Declaration of competing interest

The authors declare no potential competing interests.

Acknowledgments

We acknowledge the use of large language models, including ChatGPT and QuillBot, to support grammar correction and language refinement throughout the preparation of this manuscript.

Data availability

Not applicable. No new data were generated or analyzed.

References

[1] A.M. Blamire, MR approaches in neurodegenerative disorders, Prog. Nucl. Magn. Reson. Spectrosc. 108 (2018) 1–16, https://doi.org/10.1016/J.PNMRS.2018.11.001.
[2] S.I. Ahmad, Neurodegenerative diseases 724, Springer Science & Business Media, 2012.
[3] J.L. Cummings, J. Pillai, Neurodegenerative diseases: Unifying principles, Oxford University Press, 2016.
[4] J.P. Taylor, J. Hardy, K.H. Fischbeck, Toxic Proteins in Neurodegenerative Disease, Science 296 (5575) (2002) 1991–1995, https://doi.org/10.1126/SCIENCE.1067122.
[5] P.C. Wong, H. Cai, D.R. Borchelt, D.L. Price, Genetically engineered mouse models of neurodegenerative diseases, Nat. Neurosci. 5 (7) (2002) 633–639, https://doi.org/10.1038/nn0702-633.
[6] D.J. Selkoe, Folding proteins in fatal ways, Nature 426 (6968) (2003) 900–904, https://doi.org/10.1038/nature02264.
[7] M.A. Myszczynska, P.N. Ojamies, A.M.B. Lacoste, D. Neil, A. Saffari, R. Mead, L. Ferraiuolo, Applications of machine learning to diagnosis and treatment of neurodegenerative diseases, Nat. Rev. Neurol. 16 (8) (2020) 440–456, https://doi.org/10.1038/s41582-020-0377-8.
[8] F. Agosta, S. Galantucci, M. Filippi, Advanced magnetic resonance imaging of neurodegenerative diseases, Neurol. Sci. 38 (1) (2017) 41–51, https://doi.org/10.1007/S10072-016-2764-X/FIGURES/4.
[9] O. Hansson, Biomarkers for neurodegenerative diseases, Nat. Med. 27 (6) (2021) 954–963, https://doi.org/10.1038/s41591-021-01382-x.
[10] A. Esteva, A. Robicquet, B. Ramsundar, V. Kuleshov, M. DePristo, K. Chou, J. Dean, A guide to deep learning in healthcare, Nat. Med. 25 (1) (2019) 24–29, https://doi.org/10.1038/s41591-018-0316-z.
[11] J. van der Laak, G. Litjens, F. Ciompi, Deep learning in histopathology: the path to the clinic, Nat. Med. 27 (5) (2021) 775–784, https://doi.org/10.1038/s41591-021-01343-4.
[12] M. Wainberg, D. Merico, A. Delong, B.J. Frey, Deep learning in biomedicine, Nat. Biotechnol. 36 (9) (2018) 829–838, https://doi.org/10.1038/nbt.4233.
[13] E. Moen, D. Bannon, T. Kudo, W. Graf, M. Covert, D. Van Valen, Deep learning for cellular image analysis, Nature Metho. 16 (12) (2019) 1233–1246, https://doi.org/10.1038/s41592-019-0403-1.
[14] A. Esteva, K. Chou, S. Yeung, N. Naik, A. Madani, A. Mottaghi, R. Socher, Deep learning-enabled medical computer vision. *npj*, Digital Medicine 2021 4:1 4 (1) (2021) 1–9, https://doi.org/10.1038/s41746-020-00376-2.
[15] R. Aggarwal, V. Sounderajah, G. Martin, D.S.W. Ting, A. Karthikesalingam, D. King, A. Darzi, Diagnostic accuracy of deep learning in medical imaging: a systematic review and meta-analysis. *npj*, Digital Medicine 2021 4:1 4 (1) (2021) 1–23, https://doi.org/10.1038/s41746-021-00438-z.
[16] A. Loddo, S. Buttau, C. Di Ruberto, Deep learning based pipelines for Alzheimer's disease diagnosis: A comparative study and a novel deep-ensemble method, Comput. Biol. Med. 141 (2022) 105032, https://doi.org/10.1016/J.COMPBIOMED.2021.105032.
[17] G. Hcini, I. Jdey, H. Dhahri, Investigating Deep Learning for Early Detection and Decision-Making in Alzheimer's Disease: A Comprehensive Review, Neural. Process. Lett. 56 (3) (2024) 1–38.
[18] A. Elazab, C. Wang, M. Abdelaziz, J. Zhang, J. Gu, J.M. Gorriz, C. Chang, Alzheimer's disease diagnosis from single and multimodal data using machine and deep learning models: Achievements and future directions, Expert Syst. Appl. 124780 (2024).
[19] A. Elazab, C. Wang, M. Abdelaziz, J. Zhang, J. Gu, J.M. Gorriz, C. Chang, Alzheimer's disease diagnosis from single and multimodal data using machine and deep learning models: Achievements and future directions, Expert Syst. Appl. 124780 (2024).
[20] Y. Zhang, S. Wang, K. Xia, Y. Jiang, P. Qian, Alzheimer's disease multiclass diagnosis via multimodal neuroimaging embedding feature selection and fusion, Information Fusion 66 (2021) 170–183, https://doi.org/10.1016/J.INFFUS.2020.09.002.
[21] D. Castillo-Barnes, L. Su, J. Ramírez, D. Salas-Gonzalez, F.J. Martinez-Murcia, I. A. Illan, (DIAN), D. I. A. N, Autosomal dominantly inherited alzheimer disease: Analysis of genetic subgroups by machine learning, Information Fusion 58 (2020) 153–167, https://doi.org/10.1016/J.INFFUS.2020.01.001.
[22] N. Rahim, S. El-Sappagh, S. Ali, K. Muhammad, J. Del Ser, T. Abuhmed, Prediction of Alzheimer's progression based on multimodal Deep-Learning-based fusion and visual Explainability of time-series data, Information Fusion 92 (2023) 363–388, https://doi.org/10.1016/J.INFFUS.2022.11.028.
[23] J. Albright, Forecasting the progression of Alzheimer's disease using neural networks and a novel preprocessing algorithm, Alzheimer's & Dementia: Translational Research & Clinical Interventions 5 (1) (2019) 483–491, https://doi.org/10.1016/J.TRCI.2019.07.001.
[24] J. Bang, S. Spina, B.L. Miller, Frontotemporal dementia, Lancet 386 (10004) (2015) 1672–1682, https://doi.org/10.1016/S0140-6736(15)00461-4.
[25] J.D. Warren, J.D. Rohrer, M.N. Rossor, Frontotemporal dementia, BMJ 347 (7920) (2013), https://doi.org/10.1136/BMJ.F4827.
[26] G.D. Rabinovici, B.L. Miller, Frontotemporal lobar degeneration, CNS Drugs 24 (5) (2012) 375–398, https://doi.org/10.2165/11533100-000000000-00000.
[27] A.M. Sanford, Lewy Body Dementia, Clin. Geriatr. Med. 34 (4) (2018) 603–615, https://doi.org/10.1016/j.cger.2018.06.007.
[28] J.E. Galvin, J.E. Duda, D.I. Kaufer, C.F. Lippa, A. Taylor, S.H. Zarit, Lewy body dementia: the caregiver experience of clinical care, Parkinsonism Relat. Disord. 16 (6) (2010) 388–392.
[29] R.A.C. Roos, Huntington's disease: a clinical review, Orphanet J. Rare Dis. 5 (2010) 1–8.
[30] P. Mehta, J. Raymond, R. Punjani, M. Han, T. Larson, W. Kaye, C. Genson, Prevalence of amyotrophic lateral sclerosis in the United States using established and novel methodologies, 2017, Amyotrophic Lateral Sclerosis and Frontotemporal Degeneration 24 (1–2) (2023) 108–116.
[31] S. Subhash, N. Chaurawal, K. Raza, Promises of Lipid-Based Nanocarriers for Delivery of Dimethyl Fumarate to Multiple Sclerosis Brain, in: Neuroprotection: Method and Protocols, Springer, 2024, pp. 457–475.
[32] A. Alberdi, A. Aztiria, A. Basarab, On the early diagnosis of Alzheimer's Disease from multimodal signals: A survey, Artif. Intell. Med. 71 (2016) 1–29, https://doi.org/10.1016/J.ARTMED.2016.06.003.
[33] L. Riedl, I.R. Mackenzie, H. Förstl, A. Kurz, J. Diehl-Schmid, Frontotemporal lobar degeneration: current perspectives, Neuropsychiatr. Dis. Treat. (2014) 297–310.
[34] N.T. Bott, A. Radke, M.L. Stephens, J.H. Kramer, Frontotemporal dementia: diagnosis, deficits and management, Neurodegenerative disease management 4 (6) (2014) 439–454.
[35] L. Massimo, L.K. Evans, P. Benner, Caring for loved ones with frontotemporal degeneration: the lived experiences of spouses, Geriatr. Nurs. 34 (4) (2013) 302–306.
[36] F. Ducharme, M.-J. Kergoat, P. Antoine, F. Pasquier, R. Coulombe, The unique experience of spouses in early-onset dementia, Am. J. Alzheimers Dis. Other Dement. 28 (6) (2013) 634–641.
[37] J.C. Hanson, C.F. Lippa, Chapter 11 Lewy Body Dementia, Int. Rev. Neurobiol. 84 (2009) 215–228, https://doi.org/10.1016/S0074-7742(09)00411-5.
[38] J.P.M. Kane, A. Surendranathan, A. Bentley, S.A.H. Barker, J.-P. Taylor, A. J. Thomas, I.G. McKeith, Clinical prevalence of Lewy body dementia, Alzheimer's Res Ther 10 (2018) 1–8.
[39] J.M. Templeton, C. Poellabauer, S. Schneider, Classification of Parkinson's disease and its stages using machine learning, Sci. Rep. 12 (1) (2022) 14036.
[40] F. Cardoso, Nonmotor Symptoms in Huntington Disease, Int. Rev. Neurobiol. 134 (2017) 1397–1408, https://doi.org/10.1016/BS.IRN.2017.05.004.
[41] M.C. Kiernan, S. Vucic, B.C. Cheah, M.R. Turner, A. Eisen, O. Hardiman, M. C. Zoing, Amyotrophic lateral sclerosis, Lancet 377 (9769) (2011) 942–955, https://doi.org/10.1016/S0140-6736(10)61156-7.
[42] O. Hardiman, A. Al-Chalabi, A. Chio, E.M. Corr, G. Logroscino, W. Robberecht, L. H. Van Den Berg, Amyotrophic lateral sclerosis, Nat. Rev. Disease Primers 3 (1) (2017) 1–19, https://doi.org/10.1038/nrdp.2017.71.
[43] W. Robberecht, T. Philips, The changing scene of amyotrophic lateral sclerosis, Nat. Rev. Neurosci. 14 (4) (2013) 248–264, https://doi.org/10.1038/nrn3430.

[44] W.I. McDonald, M.A. Ron, Multiple sclerosis: the disease and its manifestations, Philos. Trans. R. Soc. Lond. B Biol. Sci. 354 (1390) (1999) 1615–1622, https://doi.org/10.1098/RSTB.1999.0506.
[45] N. Makhani, H. Tremlett, The multiple sclerosis prodrome, Nat. Rev. Neurol. 17 (8) (2021) 515–521.
[46] A.D. Korczyn, L.T. Grinberg, Is Alzheimer disease a disease? Nat. Rev. Neurol. 20 (4) (2024) 245–251.
[47] E. Mioshi, S. Hsieh, S. Savage, M. Hornberger, J.R. Hodges, Clinical staging and disease progression in frontotemporal dementia, Neurology 74 (20) (2010) 1591–1597.
[48] W. Marui, E. Iseki, T. Nakai, S. Miura, M. Kato, K. Uéda, K. Kosaka, Progression and staging of Lewy pathology in brains from patients with dementia with Lewy bodies, J. Neurol. Sci. 195 (2) (2002) 153–159.
[49] J. Chaki, M. Woźniak, Deep learning for neurodegenerative disorder (2016 to 2022): A systematic review, Biomed. Sig. Process. Control 80 (2023) 104223.
[50] G. Logroscino, B.J. Traynor, O. Hardiman, P. Couratier, J.D. Mitchell, R. J. Swingler, E. Beghi, Descriptive epidemiology of amyotrophic lateral sclerosis: new evidence and unsolved issues, J. Neurol. Neurosurg. Psychiatry 79 (1) (2008) 6–11.
[51] C.G. Goetz, Amyotrophic lateral sclerosis: early contributions of Jean-Martin Charcot, Muscle & Nerve: Offi. J. American Assoc. Electrodiagn. Medicine 23 (3) (2000) 336–343.
[52] G. Logroscino, B.J. Traynor, O. Hardiman, P. Couratier, J.D. Mitchell, R. J. Swingler, E. Beghi, Descriptive epidemiology of amyotrophic lateral sclerosis: new evidence and unsolved issues, J. Neurol. Neurosurg. Psychiatry 79 (1) (2008) 6–11.
[53] O. O'Toole, B.J. Traynor, P. Brennan, C. Sheehan, E. Frost, B. Corr, O. Hardiman, Epidemiology and clinical features of amyotrophic lateral sclerosis in Ireland between 1995 and 2004, J. Neurol. Neurosurg. Psychiatry 79 (1) (2008) 30–32.
[54] D.H. Miller, D.T. Chard, O. Ciccarelli, Clinically isolated syndromes, The Lancet Neurol. 11 (2) (2012) 157–169.
[55] F. Agosta, S. Galantucci, M. Filippi, Advanced magnetic resonance imaging of neurodegenerative diseases, Neurol. Sci. 38 (1) (2017) 41–51, https://doi.org/10.1007/S10072-016-2764-X/FIGURES/4.
[56] P. Scheltens, D. Leys, F. Barkhof, D. Huglo, H.C. Weinstein, P. Vermersch, J. Valk, Atrophy of medial temporal lobes on MRI in" probable" Alzheimer's disease and normal ageing: diagnostic value and neuropsychological correlates, J. Neurol. Neurosurg. Psychiatry 55 (10) (1992) 967–972.
[57] A. Colchester, D. Kingsley, D. Lasserson, B. Kendall, F. Bello, C. Rush, N. Stanhope, Structural MRI volumetric analysis in patients with organic amnesia, 1: methods and comparative findings across diagnostic groups, J. Neurol. Neurosurg. Psychiatry 71 (1) (2001) 13–22.
[58] A. Convit, M.J. De Leon, C. Tarshish, S. De Santi, W. Tsui, H. Rusinek, A. George, Specific hippocampal volume reductions in individuals at risk for Alzheimer's disease, Neurobiol. Aging 18 (2) (1997) 131–138.
[59] J. Ashburner, K. Friston, Multimodal image coregistration and partitioning—a unified framework, Neuroimage 6 (3) (1997) 209–217.
[60] M. Hashimoto, H. Kitagaki, T. Imamura, N. Hirono, T. Shimomura, H. Kazui, E. Mori, Medial temporal and whole-brain atrophy in dementia with Lewy bodies: a volumetric MRI study, Neurology 51 (2) (1998) 357–362.
[61] H.A.M. Middelkoop, W.M. van Der Flier, E.J. Burton, A.J. Lloyd, S. Paling, R. Barber, J.T. O'Brien, Dementia with Lewy bodies and AD are not associated with occipital lobe atrophy on MRI, Neurology 57 (11) (2001) 2117–2120.
[62] M.F. Beal, A.E. Lang, A.C. Ludolph, Neurodegenerative diseases: neurobiology, pathogenesis and therapeutics, Cambridge University Press, 2005.
[63] M. Ghaemi, R. Hilker, J. Rudolf, J. Sobesky, W.-D. Heiss, Differentiating multiple system atrophy from Parkinson's disease: contribution of striatal and midbrain MRI volumetry and multi-tracer PET imaging, J. Neurol. Neurosurg. Psychiatry 73 (5) (2002) 517–523.
[64] N. Kato, K. Arai, T. Hattori, Study of the rostral midbrain atrophy in progressive supranuclear palsy, J. Neurol. Sci. 210 (1–2) (2003) 57–60.
[65] P. Fazio, M. Paucar, P. Svenningsson, A. Varrone, Novel Imaging Biomarkers for Huntington's Disease and Other Hereditary Choreas, Curr. Neurol. Neurosci. Repor. 18 (12) (2018) 1–13, https://doi.org/10.1007/S11910-018-0890-Y/FIGURES/1.
[66] P.N. Leigh, A. Simmons, S. Williams, V. Williams, M. Turner, D. Brooks, Imaging: Mrs/mri/pet/spect: Summary, Amyotrophic Lateral Sclerosis and Other Motor Neuron Disorders 3 (sup1) (2002) S75–S80.
[67] F. Carella, M. Grisoli, M. Savoiardo, D. Testa, Magnetic resonance signal abnormalities along the pyramidal tracts in amyotrophic lateral sclerosis, Ital. J. Neurol. Sci. 16 (1995) 511–515.
[68] L.R. Peraza, J.-P. Taylor, M. Kaiser, Divergent brain functional network alterations in dementia with Lewy bodies and Alzheimer's disease, Neurobiol. Aging 36 (9) (2015) 2458–2467.
[69] S.F. Bucher, K.C. Seelos, M. Stehling, W.H. Oertel, W. Paulus, M. Reiser, High-resolution activation mapping of basal ganglia with functional magnetic resonance imaging, Neurology 45 (1) (1995) 180–182, https://doi.org/10.1212/WNL.45.1.180.
[70] P.C.M. Van Zijl, N.N. Yadav, Chemical exchange saturation transfer (CEST): what is in a name and what isn't? Magn. Reson. Med. 65 (4) (2011) 927–948.
[71] W.M. Freeze, M. van der Thiel, J. de Bresser, C.J.M. Klijn, E.S. van Etten, J.F. A. Jansen, S.J. van Veluw, CSF enhancement on post-contrast fluid-attenuated inversion recovery images; a systematic review, NeuroImage: Clinical 28 (2020) 102456.
[72] A. Varrone, K.L. Marek, D. Jennings, R.B. Innis, J.P. Seibyl, [123I] β-CIT SPECT imaging demonstrates reduced density of striatal dopamine transporters in Parkinson's disease and multiple system atrophy, Movement disorders: official journal of the Movement Disorder Society 16 (6) (2001) 1023–1032.
[73] J.J. Claus, F. van Harskamp, M.M.B. Breteler, E.P. Krenning, I. de Koning, T.J. M. Van der Cammen, D. Hasan, The diagnostic value of SPECT with Tc 99m HMPAO in Alzheimer's disease: A population-based study, Neurology 44 (3_part_1) (1994) 454.
[74] W.A. Van Gool, G.J.M. Walstra, S. Teunisse, F.M. Van der Zant, H.C. Weinstein, E. A. Van Royen, Diagnosing Alzheimer's disease in elderly, mildly demented patients: the impact of routine single photon emission computed tomography, J. Neurol. 242 (1995) 401–405.
[75] Dhawan, V., Neurology, D. E.-A. in, & 2001, undefined. (n.d.). SPECT imaging in Parkinson's disease. pascal-francis.inist.fr. Retrieved from https://pascal-francis.inist.fr/vibad/index.php?action=getRecordDetail&idt=14673161.
[76] W. Pirker, S. Djamshidian, S. Asenbaum, W. Gerschlager, G. Tribl, M. Hoffmann, T. Brücke, Progression of dopaminergic degeneration in Parkinson's disease and atypical parkinsonism: a longitudinal β-CIT SPECT study, Mov. Disord. 17 (1) (2002) 45–53.
[77] M.A. Kolanko, Z. Win, F. Loreto, N. Patel, C. Carswell, A. Gontsarova, P. A. Malhotra, Amyloid PET imaging in clinical practice, Pract. Neurol. 20 (6) (2020) 451–462.
[78] W.R.W. Martin, MR spectroscopy in neurodegenerative disease, Mol. Imaging Biol. 9 (2007) 196–203.
[79] P. Gideon, O. Henriksen, B. Sperling, P. Christiansen, T.S. Olsen, H.S. Jørgensen, P. Arlien-Søborg, Early time course of N-acetylaspartate, creatine and phosphocreatine, and compounds containing choline in the brain after acute stroke. A proton magnetic resonance spectroscopy study, Stroke 23 (11) (1992) 1566–1572.
[80] K. Nie, Y. Zhang, B. Huang, L. Wang, J. Zhao, Z. Huang, L. Wang, Marked N-acetylaspartate and choline metabolite changes in Parkinson's disease patients with mild cognitive impairment, Parkinsonism Relat. Disord. 19 (3) (2013) 329–334.
[81] U. Pilatus, C. Lais, A. de Rochmont, M. Du, T. Kratzsch, L. Frölich, K. Maurer, J. Pantel, Conversion to dementia in mild cognitive impairment is associated with decline of N-actylaspartate and creatine as revealed by magnetic resonance spectroscopy, Psychiatry Res. Neuroimaging 173 (1) (2009) 1–7.
[82] K. Nie, Y. Zhang, B. Huang, L. Wang, J. Zhao, Z. Huang, L. Wang, Marked N-acetylaspartate and choline metabolite changes in Parkinson's disease patients with mild cognitive impairment, Parkinsonism Relat. Disord. 19 (3) (2013) 329–334.
[83] W. Huang, G.E. Alexander, E.M. Daly, H.U. Shetty, J.S. Krasuski, S.I. Rapoport, M. B. Schapiro, High brain myo-inositol levels in the predementia phase of Alzheimer's disease in adults with Down's syndrome: a 1H MRS study, Am. J. Psychiatry 156 (12) (1999) 1879–1886.
[84] B. Schmitz, X. Wang, P.B. Barker, U. Pilatus, P. Bronzlik, M. Dadak, X. Ding, Effects of aging on the human brain: a proton and phosphorus MR spectroscopy study at 3T, J. Neuroimaging 28 (4) (2018) 416–421.
[85] S.G. Mueller, M.W. Weiner, L.J. Thal, R.C. Petersen, C. Jack, W. Jagust, L. Beckett, The Alzheimer's disease neuroimaging initiative, Neuroimaging Clin. N. Am. 15 (4) (2005) 869.
[86] K.P. O'Grady, S. Satish, Q.R. Owen, B.A. Box, F. Bagnato, A.J.E. Combes, S. A. Smith, Relaxation-Compensated Chemical Exchange Saturation Transfer MRI in the Brain at 7T: Application in Relapsing-Remitting Multiple Sclerosis, Front. Neurol. 13 (2022) 764690, https://doi.org/10.3389/FNEUR.2022.764690/BIBTEX.
[87] SPECT, Radiology, U of U School of Medicine, 2025. Retrieved April 1, 2025, from, https://medicine.utah.edu/radiology/research/learn/spect.
[88] G. Rizzo, M.E. Pietrolucci, G. Capece, E. Cimmino, E. Colosi, S. Ferrentino, D. Arduini, Satisfactory rate of post-processing visualization of fetal cerebral axial, sagittal, and coronal planes from three-dimensional volumes acquired in routine second trimester ultrasound practice by sonographers of peripheral centers, J. Matern. Fetal Neonatal Med. 24 (8) (2011) 1071–1076.
[89] B. Fischl, FreeSurfer, Neuroimage 62 (2) (2012) 774–781.
[90] W.D. Penny, K.J. Friston, J.T. Ashburner, S.J. Kiebel, T.E. Nichols, Statistical parametric mapping: the analysis of functional brain images, Elsevier, 2011.
[91] D.L. Beekly, E.M. Ramos, G. van Belle, W. Deitrich, A.D. Clark, M.E. Jacka, W. A. Kukull, The national Alzheimer's coordinating center (NACC) database: an Alzheimer disease database, Alzheimer Dis. Assoc. Disord. 18 (4) (2004) 270–277.
[92] D.S. Marcus, A.F. Fotenos, J.G. Csernansky, J.C. Morris, R.L. Buckner, Open access series of imaging studies: longitudinal MRI data in nondemented and demented older adults, J. Cogn. Neurosci. 22 (12) (2010) 2677–2684.
[93] K.A. Ellis, A.I. Bush, D. Darby, D. De Fazio, J. Foster, P. Hudson, P. Maruff, The Australian Imaging, Biomarkers and Lifestyle (AIBL) study of aging: methodology and baseline characteristics of 1112 individuals recruited for a longitudinal study of Alzheimer's disease, Int. Psychogeriatr. 21 (4) (2009) 672–687.
[94] T. Iwatsubo, Japanese Alzheimer's Disease Neuroimaging Initiative: present status and future, Alzheimers Dement. 6 (3) (2010) 297–299.
[95] S. Lovestone, P. Francis, K. Strandgaard, Biomarkers for disease modification trials-The innovative medicines initiative and AddNeuroMed, J. Nutr. Health Aging 11 (4) (2007) 359.
[96] C. Birkenbihl, S. Westwood, L. Shi, A. Nevado-Holgado, E. Westman, S. Lovestone, Consortium, A, ANMerge: a comprehensive and accessible Alzheimer's disease patient-level dataset, J Alzheimer's Dis 79 (1) (2021) 423–431.
[97] H. Rosen, The Frontotemporal Lobar Degeneration Neuroimaging Initiative, Center for Imaging of Neurodegenerative Diseases, 2025. Retrieved September

24, 2024, from, https://cind.ucsf.edu/research/grants/frontotemporal-lobar-degeneration-neuroimaging-initiative-0.
[98] A.L. Manera, M. Dadar, J.C. Van Swieten, B. Borroni, R. Sanchez-Valle, F. Moreno, D. Galimberti, MRI data-driven algorithm for the diagnosis of behavioural variant frontotemporal dementia, J. Neurol. Neurosurg. Psychiatry 92 (6) (2021) 608–616.
[99] K. Marek, D. Jennings, S. Lasch, A. Siderowf, C. Tanner, T. Simuni, S. Chowdhury, The Parkinson progression marker initiative (PPMI), Prog. Neurobiol. 95 (4) (2011) 629–635.
[100] J.A. Ciarochi, V.D. Calhoun, S. Lourens, J.D. Long, H.J. Johnson, H.J. Bockholt, J. A. Turner, Patterns of co-occurring gray matter concentration loss across the Huntington disease prodrome, Front. Neurol. 7 (2016) 147.
[101] S.J. Tabrizi, D.R. Langbehn, B.R. Leavitt, R.A.C. Roos, A. Durr, D. Craufurd, R. I. Scahill, Biological and clinical manifestations of Huntington's disease in the longitudinal TRACK-HD study: cross-sectional analysis of baseline data, The Lancet Neurol. 8 (9) (2009) 791–801.
[102] S.J. Tabrizi, R.I. Scahill, A. Durr, R.A.C. Roos, B.R. Leavitt, R. Jones, S.L. Hicks, Biological and clinical changes in premanifest and early stage Huntington's disease in the TRACK-HD study: the 12-month longitudinal analysis, The Lancet Neurol. 10 (1) (2011) 31–42.
[103] F.A. Wilkes, Z. Abaryan, C.R.K. Ching, B.A. Gutman, S.K. Madsen, M. Walterfang, G.F. Egan, Striatal morphology and neurocognitive dysfunction in Huntington disease: The IMAGE-HD study, Psychiatry Res. Neuroimaging 291 (2019) 1–8.
[104] S. Kalra, M. Khan, L. Barlow, C. Beaulieu, M. Benatar, H. Briemberg, A. Dionne, The Canadian ALS Neuroimaging Consortium (CALSNIC)-a multicentre platform for standardized imaging and clinical studies in ALS, MedRxiv (2020) 2020–2027.
[105] O. Commowick, A. Istace, M. Kain, B. Laurent, F. Leray, M. Simon, C. Barillot, Objective Evaluation of Multiple Sclerosis Lesion Segmentation using a Data Management and Processing Infrastructure, Sci. Report. 8 (1) (2018) 1–17, https://doi.org/10.1038/s41598-018-31911-7.
[106] M. Khojaste-Sarakhsi, S.S. Haghighi, S.M.T.F. Ghomi, E. Marchiori, Deep learning for Alzheimer's disease diagnosis: A survey, Artif. Intell. Med. 130 (2022) 102332.
[107] N. Goenka, S. Tiwari, AlzVNet: A volumetric convolutional neural network for multiclass classification of Alzheimer's disease through multiple neuroimaging computational approaches, Biomed. Sig. Process. Control 74 (2022) 103500, https://doi.org/10.1016/J.BSPC.2022.103500.
[108] R. Cuingnet, E. Gerardin, J. Tessieras, G. Auzias, S. Lehéricy, M.-O. Habert, A.D. N. Initiative, Automatic classification of patients with Alzheimer's disease from structural MRI: a comparison of ten methods using the ADNI database, neuroimage 56 (2) (2011) 766–781.
[109] M.A. Ebrahimighahnavieh, S. Luo, R. Chiong, Deep learning to detect Alzheimer's disease from neuroimaging: A systematic literature review, Comput. Methods Prog. Biomed. 187 (2020) 105242.
[110] R. Armañanzas, M. Iglesias, D.A. Morales, L. Alonso-Nanclares, Voxel-Based Diagnosis of Alzheimer's Disease Using Classifier Ensembles, IEEE Journal of Biomedical and Health Informatics 21 (3) (2017) 778–784, https://doi.org/10.1109/JBHI.2016.2538559.
[111] H.D. Tagare, C. DeLorenzo, S. Chelikani, L. Saperstein, R.K. Fulbright, Voxel-based logistic analysis of PPMI control and Parkinson's disease DaTscans, NeuroImage 152 (2017) 299–311, https://doi.org/10.1016/J.NEUROIMAGE.2017.02.067.
[112] S. Basaia, F. Agosta, L. Wagner, E. Canu, G. Magnani, R. Santangelo, M. Filippi, Automated classification of Alzheimer's disease and mild cognitive impairment using a single MRI and deep neural networks, NeuroImage: Clinical 21 (2019) 101645, https://doi.org/10.1016/J.NICL.2018.101645.
[113] G. Solana-Lavalle, R. Rosas-Romero, Classification of PPMI MRI scans with voxel-based morphometry and machine learning to assist in the diagnosis of Parkinson's disease, Comput. Methods Prog. Biomed. 198 (2021) 105793, https://doi.org/10.1016/J.CMPB.2020.105793.
[114] K. Nemoto, H. Sakaguchi, W. Kasai, M. Hotta, R. Kamei, T. Noguchi, T. Asada, Differentiating Dementia with Lewy Bodies and Alzheimer's Disease by Deep Learning to Structural MRI, J. Neuroimaging 31 (3) (2021) 579–587, https://doi.org/10.1111/JON.12835.
[115] A. Estudillo-Romero, C. Haegelen, P. Jannin, J.S.H. Baxter, Voxel-based diktiometry: Combining convolutional neural networks with voxel-based analysis and its application in diffusion tensor imaging for Parkinson's disease, Hum. Brain Mapp. 43 (16) (2022) 4835–4851, https://doi.org/10.1002/HBM.26009.
[116] H. Guan, C. Wang, J. Cheng, J. Jing, T. Liu, A parallel attention-augmented bilinear network for early magnetic resonance imaging-based diagnosis of Alzheimer's disease, Hum. Brain Mapp. 43 (2) (2022) 760–772, https://doi.org/10.1002/HBM.25685.
[117] S. Shinde, S. Prasad, Y. Saboo, R. Kaushick, J. Saini, P.K. Pal, M. Ingalhalikar, Predictive markers for Parkinson's disease using deep neural nets on neuromelanin sensitive MRI, NeuroImage: Clinical 22 (2019) 101748, https://doi.org/10.1016/J.NICL.2019.101748.
[118] S. Ahmed, B.C. Kim, K.H. Lee, H.Y. Jung, Ensemble of ROI-based convolutional neural network classifiers for staging the Alzheimer disease spectrum from magnetic resonance imaging, PLoS One 15 (12) (2020) e0242712, https://doi.org/10.1371/JOURNAL.PONE.0242712.
[119] J. Feng, S.W. Zhang, L. Chen, Extracting ROI-Based Contourlet Subband Energy Feature From the sMRI Image for Alzheimer's Disease Classification, IEEE/ACM Transactions on Computational Biology and Bioinformatics 19 (3) (2022) 1627–1639, https://doi.org/10.1109/TCBB.2021.3051177.
[120] J. Feng, S.W. Zhang, L. Chen, Extracting ROI-Based Contourlet Subband Energy Feature From the sMRI Image for Alzheimer's Disease Classification, IEEE/ACM Transactions on Computational Biology and Bioinformatics 19 (3) (2022) 1627–1639, https://doi.org/10.1109/TCBB.2021.3051177.
[121] H. Zhao, C.C. Tsai, M. Zhou, Y. Liu, Y.L. Chen, F. Huang, J.J. Wang, Deep learning based diagnosis of Parkinson's Disease using diffusion magnetic resonance imaging, Brain Imaging and Behavior 16 (4) (2022) 1749–1760, https://doi.org/10.1007/S11682-022-00631-Y/TABLES/2.
[122] D. Shi, X. Yao, Y. Li, H. Zhang, G. Wang, S. Wang, K. Ren, Classification of Parkinson's disease using a region-of-interest- and resting-state functional magnetic resonance imaging-based radiomics approach, Brain Imaging and Behavior 16 (5) (2022) 2150–2163, https://doi.org/10.1007/S11682-022-00685-Y/FIGURES/6.
[123] J. Feng, S.W. Zhang, L. Chen, Extracting ROI-Based Contourlet Subband Energy Feature From the sMRI Image for Alzheimer's Disease Classification, IEEE/ACM Transactions on Computational Biology and Bioinformatics 19 (3) (2022) 1627–1639, https://doi.org/10.1109/TCBB.2021.3051177.
[124] K. Hett, R. Giraud, H. Johnson, J.S. Paulsen, J.D. Long, I. Oguz, Patch-Based Abnormality Maps for Improved Deep Learning-Based Classification of Huntington's Disease, in: *Lecture Notes in Computer Science (including subseries Lecture Notes in Artificial Intelligence and Lecture Notes in Bioinformatics), 12267 LNCS*, 636–645, 2020, https://doi.org/10.1007/978-3-030-59728-3_62.
[125] E. Kaplan, E. Altunisik, Y. Ekmekyapar Firat, P. Datta Barua, S. Dogan, M. Baygin, U. Rajendra Acharya, Novel nested patch-based feature extraction model for automated Parkinson's Disease symptom classification using MRI images, Comput. Methods Prog. Biomed. 224 (2022) 107030, https://doi.org/10.1016/J.CMPB.2022.107030.
[126] F. Liu, S. Yuan, W. Li, Q. Xu, B. Sheng, Patch-based deep multi-modal learning framework for Alzheimer's disease diagnosis using multi-view neuroimaging, Biomed. Sig. Process. Control 80 (2023) 104400, https://doi.org/10.1016/J.BSPC.2022.104400.
[127] F. Huang, A. Qiu, Ensemble Vision Transformer for Dementia Diagnosis, in: IEEE Journal of Biomedical and Health Informatics, 2024, https://doi.org/10.1109/JBHI.2024.3412812.
[128] A. Ebrahimi, S. Luo, R. Chiong, Deep sequence modelling for Alzheimer's disease detection using MRI, Comput. Biol. Med. 134 (2021) 104537, https://doi.org/10.1016/J.COMPBIOMED.2021.104537.
[129] Y. Zhang, Q. Teng, Y. Liu, Y. Liu, X. He, Diagnosis of Alzheimer's disease based on regional attention with sMRI gray matter slices, J. Neurosci. Methods 365 (2022) 109376, https://doi.org/10.1016/J.JNEUMETH.2021.109376.
[130] R. Sharma, T. Goel, M. Tanveer, R. Murugan, FDN-ADNet: Fuzzy LS-TWSVM based deep learning network for prognosis of the Alzheimer's disease using the sagittal plane of MRI scans, Appl. Soft Comput. 115 (2022) 108099, https://doi.org/10.1016/J.ASOC.2021.108099.
[131] O. Avram, B. Durmus, N. Rakocz, G. Corradetti, U. An, M.G. Nittala, E. Halperin, Accurate prediction of disease-risk factors from volumetric medical scans by a deep vision model pre-trained with 2D scans, Nat. Biomed. Eng. 2024 (2024) 1–14, https://doi.org/10.1038/s41551-024-01257-9.
[132] T.L. Griffiths, Understanding human intelligence through human limitations, Trends Cogn. Sci. 24 (11) (2020) 873–883.
[133] J.M. Helm, A.M. Swiergosz, H.S. Haeberle, J.M. Karnuta, J.L. Schaffer, V.E. Krebs, P.N. Ramkumar, Machine learning and artificial intelligence: definitions, applications, and future directions, Curr. Rev. Musculoskelet. Med. 13 (2020) 69–76.
[134] Y. LeCun, Y. Bengio, G. Hinton, Deep learning, Nature 521 (7553) (2015) 436–444.
[135] W. Li, X. Lin, X. Chen, Detecting Alzheimer's disease Based on 4D fMRI: An exploration under deep learning framework, Neurocomputing 388 (2020) 280–287.
[136] R.J. Williams, D. Zipser, A learning algorithm for continually running fully recurrent neural networks, Neural Comput. 1 (2) (1989) 270–280.
[137] E. Amooei, A. Sharifi, M. Manthouri, Early Diagnosis of Neurodegenerative Diseases Using CNN-LSTM and Wavelet Transform, J. Healthcare Informat. Res. 7 (1) (2023) 104–124, https://doi.org/10.1007/S41666-023-00130-9/TABLES/7.
[138] A. Vaswani, Attention is all you need, in: Advances in Neural Information Processing Systems, 2017.
[139] S. Alp, T. Akan, M.S. Bhuiyan, E.A. Disbrow, S.A. Conrad, J.A. Vanchiere, M.A. N. Bhuiyan, Joint transformer architecture in brain 3D MRI classification: its application in Alzheimer's disease classification, Sci. Rep. 14 (1) (2024) 8996.
[140] K. He, X. Zhang, S. Ren, J. Sun, Deep residual learning for image recognition, in: Proceedings of the IEEE conference on computer vision and pattern recognition, 2016, pp. 770–778.
[141] K. Simonyan, A. Zisserman, Very deep convolutional networks for large-scale image recognition, arXiv preprint (2014) arXiv:1409.1556.
[142] M. Tan, Q. Le, Efficientnetv2: Smaller models and faster training, in: International conference on machine learning, PMLR, 2021, pp. 10096–10106.
[143] T. Akan, S. Akan, S. Alp, C.R. Ledbetter, M.A. Nobel Bhuiyan, AlzFormer: Video-based space-time attention model for early diagnosis of Alzheimer's disease, Neuroscience 585 (2025) 133–143, https://doi.org/10.1016/J.NEUROSCIENCE.2025.08.062.
[144] Y. LeCun, L. Bottou, Y. Bengio, P. Haffner, Gradient-based learning applied to document recognition, Proc. IEEE 86 (11) (1998) 2278–2324.
[145] A. Dosovitskiy, An image is worth 16x16 words: Transformers for image recognition at scale, arXiv preprint (2020) arXiv:2010.11929.
[146] X.W. Gao, R. Hui, Z. Tian, Classification of CT brain images based on deep learning networks, Comput. Methods Prog. Biomed. 138 (2017) 49–56, https://doi.org/10.1016/J.CMPB.2016.10.007.

[147] H. Wang, Y. Shen, S. Wang, T. Xiao, L. Deng, X. Wang, X. Zhao, Ensemble of 3D densely connected convolutional network for diagnosis of mild cognitive impairment and Alzheimer's disease, Neurocomputing 333 (2019) 145–156, https://doi.org/10.1016/J.NEUCOM.2018.12.018.
[148] N.T. Duc, S. Ryu, M.N.I. Qureshi, M. Choi, K.H. Lee, B. Lee, 3D-deep learning based automatic diagnosis of Alzheimer's disease with joint MMSE prediction using resting-state fMRI, Neuroinformatics 18 (2020) 71–86.
[149] A. Abrol, M. Bhattarai, A. Fedorov, Y. Du, S. Plis, V. Calhoun, A.D.N. Initiative, Deep residual learning for neuroimaging: an application to predict progression to Alzheimer's disease, J. Neurosci. Methods 339 (2020) 108701.
[150] S. Alinsaif, J. Lang, A.D.N. Initiative, 3D shearlet-based descriptors combined with deep features for the classification of Alzheimer's disease based on MRI data, Comput. Biol. Med. 138 (2021) 104879.
[151] J. Bae, J. Stocks, A. Heywood, Y. Jung, L. Jenkins, V. Hill, M.F. Beg, Transfer learning for predicting conversion from mild cognitive impairment to dementia of Alzheimer's type based on a three-dimensional convolutional neural network, Neurobiol. Aging 99 (2021) 53–64.
[152] M. Dong, L. Xie, S.R. Das, J. Wang, L.E.M. Wisse, R. deFlores, P.A. Yushkevich, DeepAtrophy: Teaching a neural network to detect progressive changes in longitudinal MRI of the hippocampal region in Alzheimer's disease, NeuroImage 243 (2021) 118514, https://doi.org/10.1016/J.NEUROIMAGE.2021.118514.
[153] J. Jang, D. Hwang, M3T: three-dimensional Medical image classifier using Multi-plane and Multi-slice Transformer, in: Proceedings of the IEEE/CVF conference on computer vision and pattern recognition, 2022, pp. 20718–20729.
[154] A. Alorf, M.U.G. Khan, Multi-label classification of Alzheimer's disease stages from resting-state fMRI-based correlation connectivity data and deep learning, Comput. Biol. Med. 151 (2022) 106240.
[155] S. Qasim Abbas, L. Chi, Y.P.P. Chen, Transformed domain convolutional neural network for Alzheimer's disease diagnosis using structural MRI, Pattern Recogn. 133 (2023) 109031, https://doi.org/10.1016/J.PATCOG.2022.109031.
[156] Z. Hu, Z. Wang, Y. Jin, W. Hou, VGG-TSwinformer: Transformer-based deep learning model for early Alzheimer's disease prediction, Comput. Methods Prog. Biomed. 229 (2023) 107291, https://doi.org/10.1016/J.CMPB.2022.107291.
[157] D. Agarwal, M.Á. Berbís, A. Luna, V. Lipari, J.B. Ballester, I. de la Torre-Díez, Automated medical diagnosis of Alzheimer´s disease using an efficient net convolutional neural network, J. Med. Syst. 47 (1) (2023) 57.
[158] P. He, Z. Shi, Y. Cui, R. Wang, D. Wu, A.D.N. Initiative, A spatiotemporal graph transformer approach for Alzheimer's disease diagnosis with rs-fMRI, Comput. Biol. Med. 178 (2024) 108762.
[159] Q. Chen, Q. Fu, H. Bai, Y. Hong, Longformer: longitudinal transformer for Alzheimer's disease classification with structural MRIs, in: Proceedings of the IEEE/CVF winter conference on applications of computer vision, 2024, pp. 3575–3584.
[160] S. Venkat, T. Ghodeswar, P. Chavan, S.K. Narayanasamy, K. Srinivasan, MRI-based automated diagnosis of Alzheimer's disease using Alzh-Net deep learning model, Biomed. Sig. Process. Control 102 (2025) 107367.
[161] M. Di Benedetto, F. Carrara, B. Tafuri, S. Nigro, R. De Blasi, F. Falchi, G. Amato, Deep networks for behavioral variant frontotemporal dementia identification from multiple acquisition sources, Comput. Biol. Med. 148 (2022) 105937, https://doi.org/10.1016/J.COMPBIOMED.2022.105937.
[162] A. Tiwari, A. Singhal, S.J. Shigwan, R.K. Singh, Deep Learning Framework using Sparse Diffusion MRI for Diagnosis of Frontotemporal Dementia, in: Proceedings of the IEEE/CVF International Conference on Computer Vision, 2023, pp. 3821–3827.
[163] H.D. Nguyen, M. Clément, V. Planche, B. Mansencal, P. Coupé, Deep grading for MRI-based differential diagnosis of Alzheimer's disease and Frontotemporal dementia, Artif. Intell. Med. 144 (2023) 102636, https://doi.org/10.1016/J.ARTMED.2023.102636.
[164] S. Moguilner, R. Whelan, H. Adams, V. Valcour, E. Tagliazucchi, A. Ibáñez, Visual deep learning of unprocessed neuroimaging characterises dementia subtypes and generalises across non-stereotypic samples, eBioMedicine 90 (2023), https://doi.org/10.1016/J.EBIOM.2023.104540/ATTACHMENT/1134E671-4F05-48FB-A683-602A743D43D7/MMC1.DOCX.
[165] A. Rogeau, F. Hives, C. Bordier, H. Lahousse, V. Roca, T. Lebouvier, R. Lopes, A 3D convolutional neural network to classify subjects as Alzheimer's disease, frontotemporal dementia or healthy controls using brain 18F-FDG PET, NeuroImage 288 (2024) 120530.
[166] T. Iizuka, M. Fukasawa, M. Kameyama, Deep-learning-based imaging-classification identified cingulate island sign in dementia with Lewy bodies, Sci. Report. 9 (1) (2019) 1–9, https://doi.org/10.1038/s41598-019-45415-5.
[167] K. Etminani, A. Soliman, A. Davidsson, J.R. Chang, B. Martínez-Sanchis, S. Byttner, M. Ochoa-Figueroa, A 3D deep learning model to predict the diagnosis of dementia with Lewy bodies, Alzheimer's disease, and mild cognitive impairment using brain 18F-FDG PET, Eur. J. Nucl. Med. Mol. Imaging 49 (2) (2022) 563–584, https://doi.org/10.1007/S00259-021-05483-0/TABLES/4.
[168] H. Choi, S. Ha, H.J. Im, S.H. Paek, D.S. Lee, Refining diagnosis of Parkinson's disease with deep learning-based interpretation of dopamine transporter imaging, NeuroImage: Clinical 16 (2017) 586–594, https://doi.org/10.1016/J.NICL.2017.09.010.
[169] D. Kollias, A. Tagaris, A. Stafylopatis, S. Kollias, Georgios Tagaris, Deep neural architectures for prediction in healthcare, Complex & Intelligent Syst. 4 (2) (2017) 119–131, https://doi.org/10.1007/S40747-017-0064-6.
[170] S. Shinde, S. Prasad, Y. Saboo, R. Kaushick, J. Saini, P.K. Pal, M. Ingalhalikar, Predictive markers for Parkinson's disease using deep neural nets on neuromelanin sensitive MRI, NeuroImage: Clinical 22 (2019) 101748, https://doi.org/10.1016/J.NICL.2019.101748.
[171] M.P. Adams, A. Rahmim, J. Tang, Improved motor outcome prediction in Parkinson's disease applying deep learning to DaTscan SPECT images, Comput. Biol. Med. 132 (2021) 104312.
[172] T. Vyas, R. Yadav, C. Solanki, R. Darji, S. Desai, S. Tanwar, Deep learning-based scheme to diagnose Parkinson's disease, Expert. Syst. 39 (3) (2022) e12739, https://doi.org/10.1111/EXSY.12739.
[173] K. Yasaka, K. Kamagata, T. Ogawa, T. Hatano, H. Takeshige-Amano, K. Ogaki, O. Abe, Parkinson's disease: deep learning with a parameter-weighted structural connectome matrix for diagnosis and neural circuit disorder investigation, Neuroradiology 63 (9) (2021) 1451–1462, https://doi.org/10.1007/S00234-021-02648-4/TABLES/5.
[174] B. Majhi, A. Kashyap, S.S. Mohanty, S. Dash, S. Mallik, A. Li, Z. Zhao, An improved method for diagnosis of Parkinson's disease using deep learning models enhanced with metaheuristic algorithm, BMC Med. Imaging 24 (1) (2024) 1–20, https://doi.org/10.1186/S12880-024-01335-Z/TABLES/13.
[175] H. Jiang, Y. Du, Z. Lu, B. Wang, Y. Zhao, R. Wang, G.S.P. Mok, Radiomics incorporating deep features for predicting Parkinson's disease in 123I-Ioflupane SPECT, EJNMMI Phys. 11 (1) (2024) 1–14, https://doi.org/10.1186/S40658-024-00651-1/TABLES/3.
[176] J. Yan, X. Luo, J. Xu, D. Li, L. Qiu, D. Li, C. Zhang, Unlocking the potential: T1-weighed MRI as a powerful predictor of levodopa response in Parkinson's disease, Insights into Imaging 15 (1) (2024) 1–12, https://doi.org/10.1186/S13244-024-01690-Z/FIGURES/5.
[177] M. Camacho, M. Wilms, H. Almgren, K. Amador, R. Camicioli, Z. Ismail, N. D. Forkert, Exploiting macro- and micro-structural brain changes for improved Parkinson's disease classification from MRI data, npj Parkinson's Disease 10 (1) (2024) 1–12, https://doi.org/10.1038/s41531-024-00647-9.
[178] K. Hett, R. Giraud, H. Johnson, J.S. Paulsen, J.D. Long, I. Oguz, Patch-Based Abnormality Maps for Improved Deep Learning-Based Classification of Huntington's Disease, in: *Lecture Notes in Computer Science (including subseries Lecture Notes in Artificial Intelligence and Lecture Notes in Bioinformatics), 12267 LNCS*, 636–645, 2020, https://doi.org/10.1007/978-3-030-59728-3_62.
[179] K. Guo, X. Li, X. Hu, J. Liu, T. Fan, Hahn-PCNN-CNN: an end-to-end multi-modal brain medical image fusion framework useful for clinical diagnosis, BMC Med. Imaging 21 (1) (2021) 1–22, https://doi.org/10.1186/S12880-021-00642-Z/FIGURES/15.
[180] R. Haase, N.C. Lehnen, F.C. Schmeel, K. Deike, T. Rüber, A. Radbruch, D. Paech, External evaluation of a deep learning-based approach for automated brain volumetry in patients with huntington's disease, Sci. Rep. 14 (1) (2024) 9243.
[181] I. Vernikouskaya, H.P. Müller, D. Felbel, F. Roselli, A.C. Ludolph, J. Kassubek, V. Rasche, Body fat compartment determination by encoder–decoder convolutional neural network: application to amyotrophic lateral sclerosis, Scientific Reports 2022 12:1 12 (1) (2022) 1–9, https://doi.org/10.1038/s41598-022-09518-w.
[182] R. Kushol, C.C. Luk, A. Dey, M. Benatar, H. Briemberg, A. Dionne, Y.H. Yang, SF2Former: Amyotrophic lateral sclerosis identification from multi-center MRI data using spatial and frequency fusion transformer, Comput. Med. Imaging Graph. 108 (2023) 102279, https://doi.org/10.1016/J.COMPMEDIMAG.2023.102279.
[183] S.J. Choi, S.H. Yoon, J.J. Sung, J.H. Lee, Association Between Fat Depletion and Prognosis of Amyotrophic Lateral Sclerosis: CT-Based Body Composition Analysis, Ann. Neurol. 94 (6) (2023) 1116–1125, https://doi.org/10.1002/ANA.26775.
[184] L. Coll, D. Pareto, P. Carbonell-Mirabent, Á. Cobo-Calvo, G. Arrambide, Á. Vidal-Jordana, C. Tur, Deciphering multiple sclerosis disability with deep learning attention maps on clinical MRI, NeuroImage: Clinical 38 (2023) 103376, https://doi.org/10.1016/J.NICL.2023.103376.
[185] G. Litjens, T. Kooi, B.E. Bejnordi, A.A.A. Setio, F. Ciompi, M. Ghafoorian, C. I. Sánchez, A survey on deep learning in medical image analysis, Med. Image Anal. 42 (2017) 60–88.
[186] H. Choi, S. Ha, H. Kang, H. Lee, D.S. Lee, Deep learning only by normal brain PET identify unheralded brain anomalies, EBioMedicine 43 (2019) 447–453.
[187] K.E. Keenan, M. Ainslie, A.J. Barker, M.A. Boss, K.M. Cecil, C. Charles, P. Finn, Quantitative magnetic resonance imaging phantoms: a review and the need for a system phantom, Magn. Reson. Med. 79 (1) (2018) 48–61.
[188] L. An, J. Chen, P. Chen, C. Zhang, T. He, C. Chen, A.D.N. Initiative, Goal-specific brain MRI harmonization, Neuroimage 263 (2022) 119570.
[189] S. Abbasi, H. Lan, J. Choupan, N. Sheikh-Bahaei, G. Pandey, B. Varghese, Deep learning for the harmonization of structural MRI scans: a survey, Biomed. Eng. Online 23 (1) (2024) 90.
[190] H. Guan, Y. Liu, E. Yang, P.T. Yap, D. Shen, M. Liu, Multi-site MRI harmonization via attention-guided deep domain adaptation for brain disorder identification, Med. Image Anal. 71 (2021) 102076, https://doi.org/10.1016/J.MEDIA.2021.102076.
[191] L. An, J. Chen, P. Chen, C. Zhang, T. He, C. Chen, B.T.T. Yeo, Goal-specific brain MRI harmonization, NeuroImage 263 (2022) 119570, https://doi.org/10.1016/J.NEUROIMAGE.2022.119570.
[192] M. Salmi, D. Atif, D. Oliva, A. Abraham, S. Ventura, Handling imbalanced medical datasets: review of a decade of research, Artif. Intell. Rev. 57 (10) (2024) 273.
[193] M.S. Ullah, M.A. Khan, A. Masood, O. Mzoughi, O. Saidani, N. Alturki, Brain tumor classification from MRI scans: a framework of hybrid deep learning model with Bayesian optimization and quantum theory-based marine predator algorithm, Front. Oncol. 14 (2024) 1335740, https://doi.org/10.3389/FONC.2024.1335740.
[194] Z. Chen, Z. Wang, M. Zhao, Q. Zhao, X. Liang, J. Li, X. Song, A new classification network for diagnosing Alzheimer's disease in class-imbalance MRI datasets,

Front. Neurosci. 16 (2022) 807085, https://doi.org/10.3389/FNINS.2022.807085/BIBTEX.
[195] J. Ren, N. An, C. Lin, Y. Zhang, Z. Sun, W. Zhang, H. Liu, DeepPrep: an accelerated, scalable and robust pipeline for neuroimaging preprocessing empowered by deep learning, Nat. Meth. 22 (3) (2025) 473–476, https://doi.org/10.1038/s41592-025-02599-1.
[196] J. Chaki, M. Woźniak, Deep learning for neurodegenerative disorder (2016 to 2022): A systematic review, Biomed. Sig. Process. Control 80 (2023) 104223.